EUKARYOTIC CELL, Nov. 2009, p. 1677–1691 Vol. 8, No. 11
1535-9778/09/$12.00 doi:10.1128/EC.00050-09

Reconstruction of Signaling Networks Regulating Fungal Morphogenesis by Transcriptomics▽†

Vera Meyer,[1,2]* Mark Arentshorst,[1] Simon J. Flitter,[1] Benjamin M. Nitsche,[1] Min Jin Kwon,[1] Cristina G. Reynaga-Peña,[3] Salomon Bartnicki-Garcia,[4] Cees A. M. J. J. van den Hondel,[1] and Arthur F. J. Ram[1]

Leiden University, Institute of Biology Leiden, Molecular Microbiology and Biotechnology, Kluyver Centre for Genomics of Industrial Fermentation, Sylviusweg 72, 2333 BE Leiden, The Netherlands[1]; Berlin University of Technology, Institute of Biotechnology, Department Microbiology and Genetics, Gustav-Meyer-Allee 25, D-13355 Berlin, Germany[2]; Centro de Investigacion y de Estudios Avanzados del I.P.N. Unidad Irapuato, Irapuato, Gto., 36500, Mexico[3]; and Division of Experimental and Applied Biology, Center for Scientific Investigation and Higher Education of Ensenada, Ensenada, Baja California 22860, Mexico[4]

Received 12 February 2009/Accepted 26 August 2009

Coordinated control of hyphal elongation and branching is essential for sustaining mycelial growth of filamentous fungi. In order to study the molecular machinery ensuring polarity control in the industrial fungus *Aspergillus niger*, we took advantage of the temperature-sensitive (*ts*) apical-branching *ramosa-1* mutant. We show here that this strain serves as an excellent model system to study critical steps of polar growth control during mycelial development and report for the first time a transcriptomic fingerprint of apical branching for a filamentous fungus. This fingerprint indicates that several signal transduction pathways, including TORC2, phospholipid, calcium, and cell wall integrity signaling, concertedly act to control apical branching. We furthermore identified the genetic locus affected in the *ramosa-1* mutant by complementation of the *ts* phenotype. Sequence analyses demonstrated that a single amino acid exchange in the RmsA protein is responsible for induced apical branching of the *ramosa-1* mutant. Deletion experiments showed that the corresponding *rmsA* gene is essential for the growth of *A. niger*, and complementation analyses with *Saccharomyces cerevisiae* evidenced that RmsA serves as a functional equivalent of the TORC2 component Avo1p. TORC2 signaling is required for actin polarization and cell wall integrity in *S. cerevisiae*. Congruently, our microscopic investigations showed that polarized actin organization and chitin deposition are disturbed in the *ramosa-1* mutant. The integration of the transcriptomic, genetic, and phenotypic data obtained in this study allowed us to reconstruct a model for cellular events involved in apical branching.

The formation of complex structures of multicellular organisms is a pivotal question in biology. Breaking cell symmetry has been recognized as the first step in patterning an organism. This step from apolar to polar growth involves the perception and transmission of environmental and/or internal signals and results in the formation of a cellular axis. Establishing and maintaining cell polarity are thus fundamental prerequisites for the morphogenesis of organisms. Examples for a polarized mode of cell growth can be found in yeast (budding), filamentous fungi (hyphal tip growth), algae (rhizoids), plants (root hairs and pollen tubes), and animals (neurons). As tip-growing hyphal cells provide examples of highly polarized growth, filamentous fungi are attractive eukaryotic model systems to study the mechanisms underlying this process.

In addition, filamentous fungi such as *Aspergillus niger* are also used as cell factories for the production of chemicals, pharmaceuticals, and proteins. During the last years, however, it has become clear that the morphology of filamentous fungi seriously limits the product yields obtained (37, 64, 72). Previous studies suggested a link between protein production and the abundance of actively growing hyphal tips (36, 107); however, only contradictory results have been reported so far. An increase in the number of hyphal tips has been reported to increase protein production and secretion in some cases (14, 106), whereas no correlation has been found in others (14). Thus, no generally accepted model exists so far that can be used as basis for rationally optimizing the morphology of filamentous fungi with respect to protein secretion and their rheological behavior in a bioreactor. In order to improve the morphological features of filamentous fungi in industrial processes, much more basic knowledge is required to obtain a deeper insight into the molecular networks regulating fungal morphology.

The formation of highly polarized hyphae is a defining attribute of filamentous growth. Various protein complexes (e.g., the polarisome, exocyst, and Arp2/3 complex), cytoskeletal elements, the Spitzenkörper, lipid rafts, and signaling molecules (GTPases, calcium, and cyclic AMP) are essential for establishing and maintaining polarized growth (for reviews, see references 8, 43, 44, 92, and 102). Basically, it is thought that secretory vesicles delivering proteins and cell wall material to the hyphal apex are transported along microtubules to the Spitzenkörper (8). The Spitzenkörper is a vesicle-rich region present in the apexes of fungal hyphae and defines the center

* Corresponding author. Mailing address: Leiden University, Institute of Biology, Section Molecular Microbiology and Biotechnology, Sylviusweg 72, 2333 BE Leiden, The Netherlands. Phone: 31 (0)71 5275056. Fax: 31 (0)71 5274999. E-mail: v.meyer@biology.leidenuniv.nl.

† Supplemental material for this article may be found at http://ec.asm.org/

▽ Published ahead of print on 11 September 2009.

and direction of growth (34, 35, 39, 108). The Spitzenkörper is thought to be newly formed at sites of spore germination and branch formation and is visible only in rapidly growing hyphal tips. The Spitzenkörper consists of vesicles (chitosomes, calcium-containing vesicles, and other vesicles of unknown content), proteins (F-actin, tubulin, formins, and calmodulin), and ribosomes and is viewed as a switching station from microtubule-based to actin microfilament-based vesicle transport (8–10, 20, 39, 45, 80, 92, 97, 103). Actin microfilaments focus in the center of the Spitzenkörper and organize vesicle transport to the plasma membrane (8, 19). The polarisome is a multiprotein complex adjacent to the Spitzenkörper and is thought to play a key role in the nucleation of actin microfilaments and in governing maximal polar growth rate (44, 55, 66, 102, 111). In vivo studies with strains of *Neurospora crassa* showed that three different chitin synthases concentrate in the center of the Spitzenkörper (80). Besides these known fungal polarity determinants, a kinase complex which is conserved throughout eukaryotic evolution mediates spatial control of cell growth by regulating the actin cytoskeleton. This complex, named TORC2, has been shown to be essential for the determination of cell polarity in *Saccharomyces cerevisiae*, *Dictyostelium discoideum*, and mammalian cells (47). However, such a role of TORC2 has not yet been established in any filamentous fungus.

Hyphal branching leads to mycelial development. Usually, branches arise from basal regions (lateral branching); however, new branches can also be formed by tip splitting (apical branching). The physiological details of the process of apical branching have been studied in vegetative hyphae of *A. niger*, using the temperature-sensitive hyperbranching *ramosa-1* mutant (77, 79). Four short-term events were identified: (i) cytoplasmic contraction thought to be triggered by a transient alteration of the cytoskeleton, (ii) retraction of the Spitzenkörper, (iii) disappearance of the Spitzenkörper accompanied by a sharp reduction in the hyphal elongation rate, and (iv) de novo formation of two Spitzenkörper giving rise to two apical branches. Similar events were also observed in other fungi, including wild-type *A. niger*, *Neurospora crassa*, and *Trichoderma atroviride* (78), suggesting a common mechanism for the generation of apical branches in filamentous fungi. It is believed that apical branching results from abnormal accumulation of vesicles at the tip and/or from increased tip-directed transport of vesicles, which exceeds the capacity of the leading tip. To accommodate the abnormal accumulation of the vesicles, the tip divides into two new branches (42).

Only little is known about the molecular basis of apical branching in filamentous fungi. In *N. crassa*, the *act[1]* mutant, in which actin is positioned subapically instead of apically, displays increased tip splitting (101). Furthermore, the *spray* mutant (with altered intracellular calcium distribution) and the *frost* mutant (with disturbed manganese homeostasis) showed excessive apical-branching phenotypes (15, 90). In a large-scale genetic screen for morphological mutants of *N. crassa*, more proteins whose mutations led to hyphal tip splitting were identified (87), e.g., Ypk1, an ortholog of the yeast and nematode TORC2 effector proteins Ypk1p and SGK-1, and Cdc24, an activator protein of the GTPase Cdc42 (49, 50, 87). A requirement for Cdc42 in tip splitting was also supported by observations of the filamentous yeast *Ashbya gossypii* (85). Other proteins reported to be specifically required for apical branching in *A. gossypii* are the protein kinase AgCla4p, the paxillin-like protein AgPxl1p, and the polarisome components AgSpa2p and AgBni1p (5, 55, 56, 85). Congruently, mutations in the AgBni1p ortholog SepA evoked increased apical branching in *Aspergillus nidulans* (89).

TABLE 1. Strains used in this study

Strain	Description	Source or reference
A. niger		
N402	Wild type	Lab collection
AB4.1	*pyrG*$^-$	98
MA70.15	Δ*kusA pyrG*$^-$	65
T312	Wild type	77
ramosa-1 mutant	Mutant of T312 obtained after UV mutagenesis	77
14, 17	Heterokaryotic strain, Δ*rmsA*	This work
S. cerevisiae		
26474	*Mat***a**/α *his3Δ1/his3Δ1 leu2Δ0/leu2Δ0 met15Δ0/MET15 lys2Δ0/LYS2 ura3Δ0/ura3Δ0* YOL078w/Yol078w::Kan^r	Research Genetics
ARY1	26474 containing pGal1-RmsA	This work
ARY2	26474 containing pGal1-Avo1	This work
ARY1.1B	Segregant from ARY1, ΔYol078w, pGal-RmsA	This work
ARY2.4B	Segregant from ARY2, ΔYol078w, pGal-Avo1	This work
ARY2.4C	Segregant from ARY2, pGal-Avo1	This work

In order to understand the molecular basis for apical branching in *A. niger*, we have identified and characterized the genetic locus affected in the *ramosa-1* mutant. Here, we report that a single point mutation in the *rmsA* gene (An02g04280) is responsible for the mutant phenotype of the *ramosa-1* mutant. The RmsA protein is homologous to the Avo1p/Sin1 protein, which is conserved from yeast to humans and, as a component of the TORC2 complex, is involved in regulating actin cytoskeleton polarity (104, 110). We show that RmsA serves as a functional equivalent of Avo1p and has a pivotal role in polarity maintenance in *A. niger*. We furthermore present for the first time a transcriptomic fingerprint of apical branching, which enabled us to obtain valuable mechanistic insights into the signaling machinery controlling morphogenesis of *A. niger*.

MATERIALS AND METHODS

Strains, culture conditions, and molecular techniques. The *A. niger* and *S. cerevisiae* strains used in this study are listed in Table 1. *Escherichia coli* strain XL1-Blue served as the host for all plasmid work. General cloning procedures in *E. coli* were done as described by Sambrook and Russel (82). *A. niger* strains were cultivated in minimal medium (13) containing 1% glucose as a carbon source or in complete medium, consisting of minimal medium supplemented with 1% yeast extract and 0.5% Casamino Acids; 10 mM uridine was added when required.

Fermentation medium (FM) is composed of 0.75% glucose, 0.45% NH_4Cl, 0.15% KH_2PO_4, 0.05% KCl, 0.05% $MgSO_4$, 0.1% salt solution (13), and 0.003% yeast extract. The pH of FM was adjusted to 3. *S. cerevisiae* strains were cultivated in yeast extract-peptone (YP) medium containing either 1% glucose or 1% galactose as a carbon source. Transformation of *A. niger* strains was conducted as described earlier (75). *S. cerevisiae* genetic methods as described by Guthrie and Fink (40) were used.

Bioreactor cultivation. Freshly harvested conidia (5×10^9) from strain T312 and the *ramosa-1* mutant were used to inoculate 5 liters of FM. Cultivations were performed in a BioFlo3000 bioreactor (New Brunswick Scientific), where the temperature, pH (set to 3), and agitation speed were controlled online using the program NBS Biocommand. The cultivation program followed four consecutive phases: (i) 24°C, agitation speed of 250 rpm, and headspace aeration for 13 h; (ii) 37°C, agitation speed of 750 rpm, and sparger aeration for 4 h; (iii) 25°C, agitation speed of 750 rpm, and sparger aeration for 3 h; and (iv) 37°C, agitation speed of 750 rpm, and sparger aeration for 1 h. Mycelial samples were taken after certain time points for microarray and microscopic analyses (see below).

Identification and cloning of *rmsA*. The *rmsA* gene was identified by complementation of the temperature-sensitive phenotype of the *ramosa-1* mutant using the cosmid library pAOpyrGcosArp containing genomic DNA of wild-type *A. niger* (kindly provided by F. Schuren and P. Punt, TNO Nutrition). The complementing plasmid isolated was named pRamosa-13. Restriction analysis revealed that pRamosa-13 contained a 9-kb NcoI fragment as well as a 3.4-kb ClaI/NcoI fragment that were each fully capable of complementing the *ramosa-1* mutant phenotype. The 9-kb NcoI fragment and the 3.4-kb ClaI/NcoI fragment were cloned into pUC21 (100), giving pRamosa-18 and pRamosa-19, respectively. Double-stranded DNA sequencing of pRamosa-18 revealed that the 9-kb insert harbored a 2,683-bp-long open reading frame (ORF) that was designated *rmsA*.

Deletion of *rmsA*. To construct an *rmsA* deletion plasmid, pRamosa-18 was digested with NotI and KpnI to obtain a 6-kb fragment containing the 5′ region of the *rmsA* gene. A 0.7-kb fragment containing the 3′ flanking region of the *rmsA* gene was obtained using a XhoI/NotI double restriction of pRamosa-19. A 2.5-kb KpnI/SalI fragment containing the *Aspergillus oryzae pyrG* gene was obtained from pAO4-13 (29). Three-way ligation of these fragment resulted in the disruption plasmid pΔ*rmsA*. Before transformation into *A. niger* strain AB4.1 or MA70.15, pΔ*rmsA* was linearized using BglII. Disruption of the *rmsA* gene in *A. niger* was analyzed by Southern blot analysis. Genomic DNAs of putative Δ*rmsA* strains and a wild-type strain were isolated and digested with ClaI. As a probe, a 718-bp XhoI/NcoI *rmsA* fragment that was labeled by the random-priming method using [α-^{32}P]dATP was used. Hybridizations were carried out at 65°C.

The heterokaryon rescue technique (71) was used to show that *rmsA* encodes an essential protein. Conidiospores from primary *rmsA* transformants in the MA70.15 (Δ*kusA*) background were analyzed for growth on selective medium (lacking uridine). Conidiospores from transformants that did not grow on selective medium (16 out of the 23 primary transformants) were considered potential heterokaryons, which was confirmed by Southern blot analysis. Southern blot analysis of transformants that produced viable conidiospores showed that they had the *rmsA* deletion construct integrated ectopically.

Complementation of Δ*AVO1* in *S. cerevisiae*. Plasmid pYES2 (Invitrogen) was used for the expression of *AVO1* (Yol078w) and *rmsA* under the control of the inducible *GAL1* promoter. The 3,531-bp fragment containing the *AVO1* gene was amplified using primers pYol078P1 and pYol078P2 with *S. cerevisiae* genomic DNA as a template and cloned using SstI/XbaI restriction sites into pYES2, giving plasmid pGal-Avo1. The 2,535-bp fragment containing the *rmsA* cDNA was amplified using primers pRamosa23 and pRamosaP24 with genomic cDNA of *A. niger* (N402) (kindly provided P. Punt, TNO Quality of Life) as a template and cloned into pYES2 using SstI and XbaI, yielding plasmid pGal-RmsA. The *AVO1*/Yol078w heterozygote deletion strain in the BY4743 background was obtained from Research Genetics and transformed with pGal-Avo1 or pGal-RmsA using the *URA3* selection marker. Transformants were grown selectively, induced for sporulation, and subjected to tetrad analysis as described previously (40).

Microarray and Northern analyses. Culture broth (400 ml each) obtained from the above-described bioreactor cultivations were quickly harvested via filtration, and mycelial samples were immediately frozen using liquid nitrogen. Total RNA extraction, RNA quality control, labeling, Affymetrix microarray chip hybridization, scanning, and signal calculation (P, present; M, marginal; A, absent) were performed as previously described (67). Microarray analyses for T312 and the *ramosa-1* mutant were performed on cells obtained from three independent bioreactor cultivations (biological triplicate).

Expression data were analyzed using the program GeneSpring 7.3. (Agilent Technologies). For normalization, default settings were used (50th percentile per chip, median per gene). Genes were defined as being differentially expressed if their expression levels varied at least 1.5-fold in the *ramosa-1* samples compared to T312 and if the difference was statistically significant (Student's *t* test, *P* value cutoff of 0.05).

Northern analyses using 5 μg RNA from each strain were performed as described earlier (67). For hybridizations, PCR amplicons which were obtained by using the respective primer pairs as listed in Table S1 in the supplemental material were used. For 18S rRNA hybridization, a 2-kb BglII fragment from plasmid pMN1 (18) was used as probe.

Staining procedures and microscopy. Actin immunostaining and calcofluor white (CFW) and DAPI (4′,6′-diamidino-2-phenylindole) staining of T312 and *ramosa-1* germlings were performed as described previously (41, 66, 68). For actin immunostaining, the protocol used included two modifications as described earlier (68): lysing enzyme from Sigma was used for cell wall digestion, and the monoclonal antibody against actin was obtained from MP Biomedicals. For detection of intracellular reactive oxygen species (ROS), a protocol based on nitroblue tetrazolium (NBT) staining (51) was slightly modified as follows. Germlings of both strains were incubated in 50 mM sodium phosphate buffer containing 0.5 mg/ml NBT for 1 h, washed once each with 100% methanol and sterile water, and immediately subjected to microscopy. Microscopic pictures were captured using an Axioplan 2 instrument (Zeiss) equipped with a DKC-5000 digital camera (Sony). Both light (using differential interference contrast settings) and fluorescence (using green fluorescent protein or DAPI settings) images were captured with 40× or 100× objectives. Images were processed using Adobe Photoshop 6.0 (Adobe Systems Inc.).

Bioinformatics. Responsive genes of the *ramosa-1* mutant were functionally classified into FunCat categories as described previously (81). In order to perform gene set enrichment analysis (www.broadinstitute.org/gsea/) (93), expression values were computed using robust multiarray analysis (48). Gene sets based on FunCat categories were generated on a genome-wide scale, whereby the proportion of false positives was controlled by calculating the false discovery rate (< 0.05) according to the method of Benjamini and Hochberg (12). In silico analysis of putative transcription factor binding sites localized in the 1,000-bp upstream regions of *A. niger* genes was performed using an in-house-developed Perl script named the transcription factor binding site finder (TFBSF). The upstream regions were extracted for 13,750 out of 14,165 ORFs using the annotated genome sequence of *A. niger* strain CBS 513.88 (73). Upstream regions of 415 ORFs could not be identified due to contig borders or incorrectly determined ORFs (missing start codon). The upstream regions of the differentially expressed genes of the *ramosa-1* mutant were searched for the presence of putative binding sites recognized by 25 known transcription factors from *Aspergillus* or *Trichoderma* species (see Table S3 in the supplemental material). Furthermore, these sequences were screened for the presence of common but so-far-undescribed putative binding motifs using the motif-based sequence analysis tool (MEME [6] at http://meme.nbcr.net/meme4_1/intro.html).

To determine significant over- or underrepresentation of binding sites, the background distribution of the identified motifs was determined via bootstrapping. For the up- and downregulated sets of genes, 500,000 bootstraps were performed separately. Out of the available 13,750 extracted upstream regions, random sets of equal size as the two sets of interest were selected and the presence of putative binding sites was determined. The average results for these bootstraps were interpreted as the background distribution. The probabilities of an over- or underrepresentation of putative binding sites of a transcription factor of equal or greater extent compared to the requested set was interpreted as the *P* value.

Microarray data accession number. The microarray data have been deposited at GEO (http://www.ncbi.nlm.nih.gov/geo/) under accession number GSE17641.

RESULTS

The apical-branching phenotype of the *ramosa-1* mutant is reversible. Previous studies have characterized the phenotype of the *ramosa-1* mutant and its respective wild-type strain T312 using mature vegetative hyphae. Hyphae of the *ramosa-1* mutant developed apical branches when subjected to a restrictive temperature (34 to 40°C), whereas at a permissive temperature (23°C), the *ramosa-1* phenotype was similar to that of the wild-type strain (79). In this study, we questioned whether this observation is also valid for young germlings of the *ramosa-1* mutant. In order to ensure controlled and equal growth conditions, we cultivated spores of both strains in a bioreactor using a defined temperature program (see below). As followed by the dissolved oxygen tension, equal growth behavior was observed for the *ramosa-1* mutant and T312 for the first 17 h of cultivation (data not shown).

First, spores of both strains were inoculated at 24°C and allowed to germinate for 13 h. After initial swelling, the majority of the spores (>90%) of both strains formed unbranched germ tubes and displayed indistinguishable phenotypes (Fig.

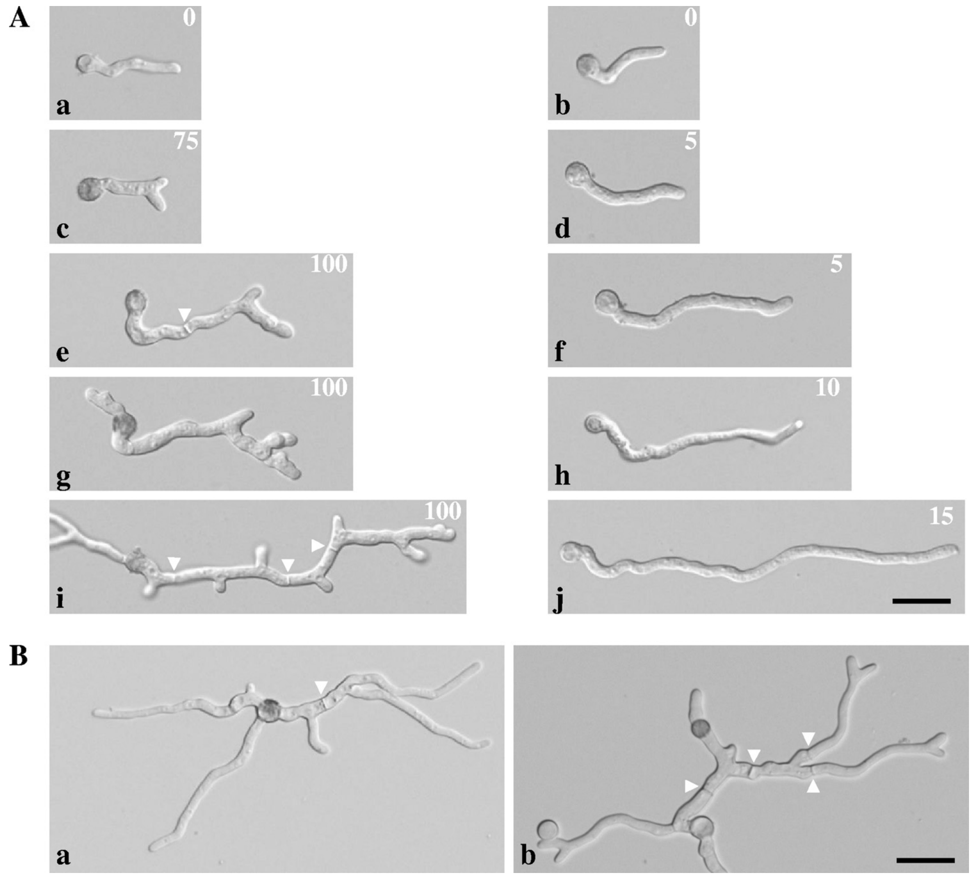

FIG. 1. Manipulation of polarized growth in the *ramosa-1* mutant. (A) Conidia obtained from the *ramosa-1* and T312 strains were cultivated under controlled conditions and subjected to differential interference contrast microscopy. Pictures for at least 100 germlings were taken for each time point and the percentage of branched germlings calculated (number at upper right). Young unbranched germlings are visible for both strains after 13 h of growth at 24°C (a and b). After a temperature upshift to 37°C for 1 h, 75% of *ramosa-1* germlings show apical branches (c), compared to only 5% of T312 germlings (d). For the next 3 hours at 37°C, 100% of *ramosa-1* germlings developed additional apical and subapical branches (e, g, and i) before growth ceased (i). In contrast, the majority of T312 germlings grew in a polar fashion (f, h, and j). (B) Polar growth of *ramosa-1* germlings corresponding to panel i resumed after the temperature was downshifted to 24°C for 3 h (a). A subsequent temperature upshift to 37°C for 1 h resulted in the formation of new apical branches (b). Septa are indicated by arrowheads. Bars, 10 μm.

1A, panels a and b). After this phase, the temperature was set to the restrictive temperature of 37°C for a period of 4 h. Within the first hour, already 75% of *ramosa-1* germlings had started to develop apical branches, whereas germlings of T312 continued elongating with no branching (Fig. 1A, panels c and d). During further cultivation at 37°C, the majority of T312 germlings grew in an apical fashion, and lateral branches were only rarely observed (Fig. 1A, panels f, h, and j). In contrast, all germlings of the *ramosa-1* mutant displayed apical branches, and newly formed tips branched again (usually one of the two apical tips branched apically), suggesting that the ability of *ramosa-1* germlings to maintain stable polarity axes is limited to a short period, after which new polarity axes become established via apical branching. Cultivation at the restrictive temperature also produced increased septation and subapical branches next to the septa (Fig. 1A, panels e, g, and i). However, when the temperature was shifted back to the permissive temperature (24°C) and kept there for the next 3 h of cultivation, *ramosa-1* germlings regained their ability to elongate without producing apical branches; i.e., they maintained stable polarity axes (Fig. 1B, panel a). This observation indicated that the morphogenetic program of the *ramosa-1* mutant can be manipulated by simply altering the ambient growth temperature. Indeed, after an additional upshift to 37°C for 1 hour, new polarity axes became established (Fig. 1B, panel b). Thus, establishment and (re)maintenance of new polarity axes can be induced or repressed in *ramosa-1* germlings.

RmsA shows homology to Avo1p/Sin1 proteins. To identify the genetic locus responsible for the mutant phenotype of the *ramosa-1* mutant, a complementation approach was followed. When cultivated on solid medium at 37°C, the *ramosa-1* mutant has a drastically reduced radial colony growth rate and forms small, very compact colonies lacking conidiophores and conidia (79). A cosmid library was transformed to the *ramosa-1* mutant, and transformants were selected based on their ability to grow and conidiate at 37°C (data not shown). The isolation and subsequent sequencing of the complementing plasmid pRamosa-18 resulted in the identification of a single ORF, designated *rmsA*.

The 2,683-bp-long ORF is interrupted by two introns, the positions of which were confirmed by sequencing of the corresponding cDNA. As depicted in Fig. S1 in the supplemental

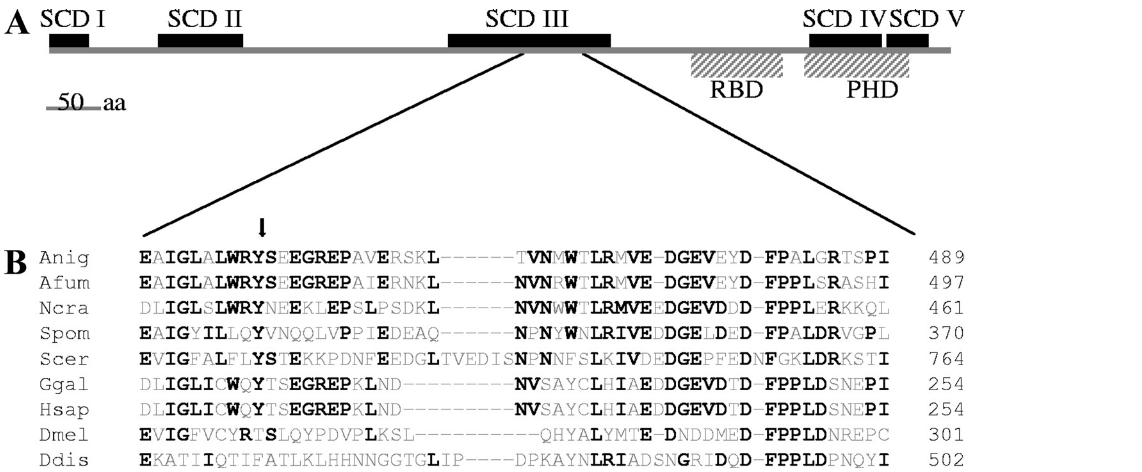

FIG. 2. Alignment of RmsA and its ortholog proteins. (A) Schematic representation of the domains present in RmsA. (B) A region within the SCD III domain showing highest homology between the orthologous proteins. Amino acids that are identical in at least four species are highlighted in bold. The tyrosine residue that has been exchanged in RmsA present in the *ramosa-1* mutant is indicated by an arrow. Anig, *Aspergillus niger* RmsA (GenBank accession number An02g04280); Afum, *Aspergillus fumigatus* Sin1 (XP_755553); Ncra, *Neurospora crassa* Sin1 (XP_322410); Spom, *Schizosaccharomyces pombe* Sin1 (NP_59470); Scer, *Saccharomyces cerevisiae* Avo1 (NP_014563); Hsap, *Homo sapiens* MAPKAP1 (BC002326); Ggal, *Gallus gallus* Sin1 (AF153127); Ddis, *Dictyostelium discoideum* RipA (XP_638477); Dmel, *Drosophila melanogaster* (AAF58247).

material, the deduced 838-amino-acid sequence of RmsA shows a high degree of homology to the Avo1p/Sin1 protein family. In *Saccharomyces cerevisiae*, Avo1p (*a*dheres *vo*raciously to TOR2) has been shown to be an interactor with the TOR (target of rapamycin) protein complex (TORC2), which is necessary for the polarization of the actin cytoskeleton (61). The *Schizosaccharomyces pombe rmsA* ortholog Sin1 was originally reported to interact with the mitogen-activated protein (MAP) kinase StyI (105); however, most recently, it has also been described as an essential component of TORC2 (46).

Avo1p/Sin1 proteins, in general, are highly conserved in metazoan species and fungi (104). Five regions with considerable identity (SCDs I to V) have been identified in Avo1p/Sin1 orthologous proteins (104) and are also present in the RmsA protein (SCD I, amino acids [aa] 1 to 39; SCD II, aa 104 to 180; SCD III, aa 369 to 517; SCD IV, aa 702 to 767; SCD V, aa 768 to 816) (Fig. 2A). Schroder et al. have additionally identified two putative domains within most Avo1p/Sin1 orthologs, namely, a Raf-like Ras binding domain and a pleckstrin homology domain (86), which were also identified in RmsA (Ras binding domain, aa 594 to 677; pleckstrin homology domain, aa 699 to 789) (Fig. 2A). Sequence comparison of the *rmsA* genes in T312 and the *ramosa-1* mutant revealed a single point mutation, resulting in an exchange of a highly conserved tyrosine for asparagine at aa 447 (Fig. 2B). Remarkably, this mutation localized within region SCD III, which shows greatest conservation in metazoa and fungi (104).

Deletion of the *rmsA* gene is lethal. To investigate the consequences of a loss of function of the *rmsA* gene in *A. niger*, a gene deletion vector (pΔ*rmsA*) was constructed, in which an internal part of the *rmsA* ORF was replaced by the *pyrG* selection marker from *A. oryzae*. The wild-type strain AB4.1 (*pyrG*$^{-}$) was repeatedly transformed with pΔ*rmsA*; however, all attempts to detect any transformants deleted for *rmsA* failed, suggesting that the gene is, similarly to its *S. cerevisiae* counterpart *AVO1*, essential. This assumption was confirmed by using strain MA70.15 (Δ*kusA*, *pyrG*$^{-}$) as the recipient strain. This strain has been shown to be valuable for the generation of balanced heterokaryons in primary transformants (65). Southern blot analysis of primary transformants obtained with strain MA70.15 proved the heterokaryotic nature of selected transformants; i.e., the hybridization patterns were congruent with the presence of the wild-type and *rmsA*-deleted genes, respectively (see Fig. S2 in the supplemental material). Conidia derived from these heterokaryotic transformants failed to grow under selective conditions (medium lacking uridine), supporting the conclusion that the *rmsA* gene is essential in *A. niger*. To test whether the *rmsA* deletion was essential at different temperatures or could be suppressed by high-osmolarity medium, spores from the heterokaryotic Δ*rmsA* 17 strain were plated at different growth temperatures (25°C, 32°C, and 37°C) or in high-osmolarity medium (1.2 M sorbitol or 0.6 M KCl). None of these conditions allowed growth on selective medium, indicating that these conditions could not rescue the *rmsA* deletion.

RmsA complements the *AVO1* null phenotype of *S. cerevisiae*. The RmsA ortholog Avo1p is an essential protein in *S. cerevisiae* (61). In order to get a first insight into the function of RmsA, a heterozygous *AVO1*::*kanMX4*/*AVO1 S. cerevisiae* strain was transformed with a plasmid that contained the *rmsA* wild-type gene under the control of the *S. cerevisiae GAL1* promoter (plasmid pGal-RmsA). As controls, the recipient strain was transformed with the *S. cerevisiae AVO1* gene under the control of the same promoter (plasmid pGal-Avo1) and with the empty plasmid (pYES2). Transformed diploid cells were allowed to sporulate, and haploid spores were dissected on galactose plates. The analysis confirmed that *AVO1* is an essential gene, as only two viable spores per tetrad were obtained after dissecting *avo1*/*AVO1* heterozygote stains containing the empty pYES2 plasmid. Dissection of the *avo1*/*AVO1* diploid strain containing pGal-Avo1 resulted in four viable spores, and subsequent analysis showed that expression of

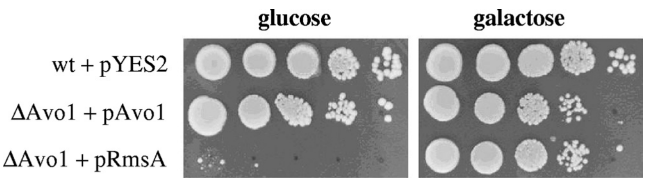

FIG. 3. Complementation of *AVO1* deletion with the *rmsA* gene in *S. cerevisiae*. Cell suspensions of *S. cerevisiae* strains were spotted onto solid YP-glucose or YP-galactose medium and inoculated for 3 days at 28°C. Cells were spotted in a 10-fold dilution series starting with $\sim 1 \times 10^5$ cells as the highest concentration. Note that the *GAL1* promoter allows leaky expression under noninduced conditions (glucose). wt, wild type.

AVO1 from the *GAL1* promoter could rescue the *avo1* deletion on both galactose and glucose media (Fig. 3). The *rmsA* gene was also fully competent in rescuing the loss of *AVO1* function, indicating that RmsA is a functional homolog of Avo1p. However, complementation was obtained only on galactose medium, indicating that high levels of *rmsA* are required for full complementation. *S. cerevisiae* wild-type strains derived from dissecting the *avo1*/*AVO1* heterozygote diploid strain containing the plasmid pGal-RmsA or pGal-Avo1, respectively, did not result in any altered phenotype compared to the wild-type situation (data not shown), suggesting that overexpression of Avo1p or RmsA is not detrimental to *S. cerevisiae*.

Mutation of RmsA results in actin and chitin depolarization. Avo1p has been described to be essential for the maintenance of TORC2 integrity in *S. cerevisiae* (109). TORC2 is a protein complex that is required for actin polarization, thereby mediating spatial control of cell growth, as well as for positive regulation of the cell wall integrity (CWI) pathway via activation of Rom2p, a GDP/GTP exchange factor for Rho1p (28, 84). We assumed that if a similar complex existed in *A. niger* and had the same function, actin localization and cell wall organization would be disturbed in the *ramosa-1* mutant when grown at 37°C due to a nonfunctional (or partially functional) $RmsA^{Y447N}$ protein.

We thus visualized actin via immunofluorescence and chitin via CFW staining in *ramosa-1* and T312 germlings shifted for 4 h to the restrictive temperature (similar to those in panels i and j in Fig. 1A). As depicted in Fig. 4, actin localization differed in *ramosa-1* germlings compared to the wild-type situation. Actin patches were highly clustered at the apex, i.e., at the extreme tip, in 42 out of 49 hyphal tips analyzed from wild-type germlings (85.7%) (Fig. 4c). In seven hyphal tips (14.3%), we could observe a faint actin spot at the apex together with actin patches behind the apex (Fig. 4d). These patches presumably form a cortical actin ring corresponding to the actin collar most recently observed in mature hyphae of *A. nidulans* by time-lapse microscopy (94). In comparison, only 21 out of 68 hyphal tips (30.4%) from the *ramosa-1* mutant displayed a considerable congregation of actin patches at the hyphal apex (similar to that shown in Fig. 4c), and in only three of these could we detect a basal actin collar (similar to that in Fig. 4d). In the majority of *ramosa-1* tips analyzed (69.6%), however, actin patches were scattered randomly along the subapex (Fig. 4a and b), resembling the actin delocalization effect of the actin-depolymerizing agent cytochalasin A in *A. nidulans* (94) and the localization pattern of actin in the act^1 mutant of *N. crassa* (101).

Actin polarization at the hyphal tip has been shown to be required for polarized chitin synthesis in *A. nidulans* (95). This observation might also hold true for *A. niger*, as chitin was found to be accumulated at the hyphal apex in wild-type germlings (Fig. 4f). This cap-like distribution, however, was not present in *ramosa-1* germlings (Fig. 4e), suggesting that loss of actin polarization in the *ramosa-1* mutant distorts chitin synthesis at the hyphal tip. Remarkably, the overall CFW fluorescence was found to be much stronger for *ramosa-1* germlings than for T312 germlings (Fig. 4g and h), possibly hinting at a higher chitin abundance in the cell walls of the *ramosa-1* mutant, which is in accordance with the previous finding that disappearance of the Spitzenkörper during apical branching is accompanied by considerable cell wall thickening (77).

No differences between *ramosa-1* and wild-type germlings were observed when they were subjected to DAPI staining. The nuclear distributions, i.e., a regular spacing between nuclei, were similar in both strains (data not shown). Likewise, staining for ROS, described to be required for polarized growth of plant organs (22) and fungi (88), did not reveal any obvious discrepancies between the two strains. A tip-localized accumulation of ROS was found for the *ramosa-1* mutant and T312 (Fig. 4i and j).

Gene expression profiling in the *ramosa-1* mutant induced for apical branching. Microarray analyses were performed using RNA samples obtained from each three bioreactor runs (biological triplicate) of the *ramosa-1* mutant and T312 (negative control). To analyze early events in apical branching, germlings (corresponding to panels c and d in Fig. 1A) were harvested 1 h after the temperature upshift to 37°C. Microarray data were processed as described in Materials and Methods, and genes showing at least 1.5-fold-higher or -lower expression in the *ramosa-1* mutant were evaluated as being differentially expressed. Expression of 136 genes out of 14,165 *A. niger* genes was modulated, and 109 thereof displayed increased expression levels in the *ramosa-1* strain. A comprehensive list of all differentially expressed genes is depicted in Table S2 in the supplemental material. Gene orthologs which have been shown to be important for polar growth in *N. crassa* (52, 87) are indicated there. In order to validate the changes in gene expression, Northern analyses for 13 selected genes were performed using the same RNA samples as utilized for the microarray analyses. As shown in Fig. 5, the Northern data are in good agreement with the microarray data; i.e., genes showing high or low levels of differential expression in the *ramosa-1* mutant displayed comparable signals of intense or modest upregulation (or downregulation) in the Northern experiment.

Functional classification of all responsive genes of the *ramosa-1* mutant into FunCat categories (81) revealed that the category with the largest number of differentially expressed genes is that of genes involved in metabolism (Table 2). Apical branching of the *ramosa-1* mutant has been reported to be accompanied by substantial reduction of the elongation rate of the parent hypha prior to appearance of apical branches (77). A possible explanation for this observation might be diminished ATP production as a result of reduced glucose uptake caused by decreased expression of An09g04810 (predicted glucose transporter) and a switch to anaerobic energy generation

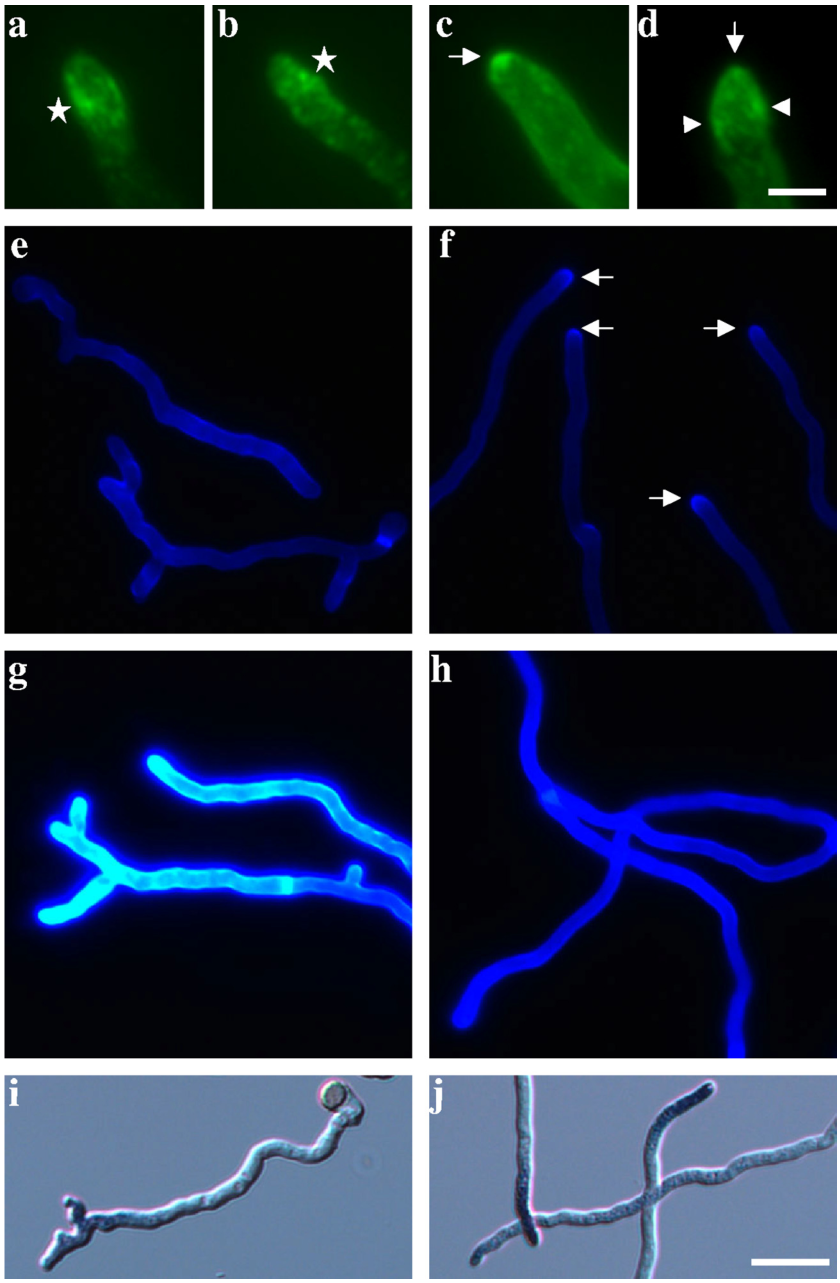

FIG. 4. Phenotypic analysis of *ramosa-1* and T312 germlings. Samples were taken after cultivation for 13 h at 24°C, followed by cultivation for 4 h at 37°C. Microscopic pictures were taken for at least 50 germlings from each strain, and representative pictures are shown. (a to d) Actin immunostaining of the *ramosa-1* mutant (a and b) and T312 (c and d). Polarized actin localization is indicated by arrows, an actin collar by arrowheads, and depolarized actin patches by stars. (e to h) CFW staining of the *ramosa-1* mutant (e and g) and T312 (f and h). Pictures for panels e and f were taken using an automatic exposure time, and pictures for panels g and h were taken using a 100-ms exposure time. Polarized chitin localization as visible in panel f is indicated by arrows. The increase in CFW fluorescence intensity in panel g suggests enhanced chitin levels at *ramosa-1* cell walls. (i and j) Microscopic images of the *ramosa-1* mutant (i) and T312 (j) stained with NBT. The presence of ROS is reflected by blue hyphal tips. Bars, 5 μm for panels a to d and 10 μm for panels e to j.

reflected by increased transcription of genes encoding a pyruvate decarboxylase (An02g06820) and a alcohol dehydrogenase (An02g02060) (Table 3).

Within the category of metabolism, genes coding for proteins involved in glutamate metabolism (An11g07960 coding for glutaminase and An02g14590 coding for a NAD^+-dependent glutamate dehydrogenase) were upregulated (Table 3 and Fig. 6). Most interestingly, deletion of the NADPH-dependent glutamate dehydrogenase results in reduced branching frequencies in *A. nidulans* and *Penicillium chrysogenum* (96). Glutamate is one of the main cellular precursors used for the synthesis of other amino acids, suggesting that amino acid starvation might be sensed in the *ramosa-1* mutant. Alternatively, glutamate might have been used to fuel the citrate cycle

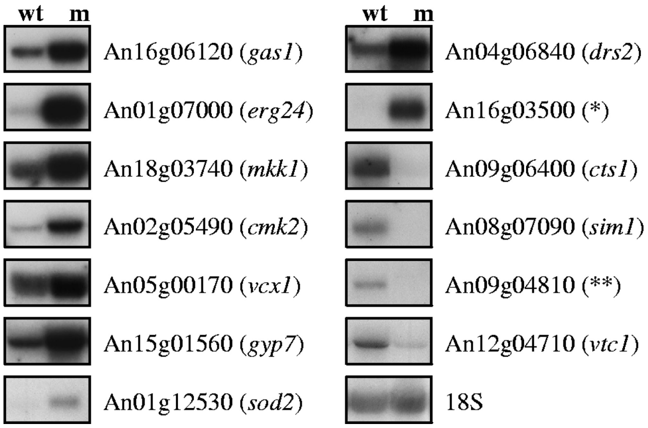

FIG. 5. Northern analysis of selected genes differentially expressed in the *ramosa-1* mutant. Five micrograms of RNA was loaded onto each lane (wt, T312; m, *ramosa-1* mutant) and hybridized with different probes as indicated. Control hybridization with 18S RNA confirmed equal loading. Gene names given in parentheses refer to the closest *S. cerevisiae* homolog (Table 3), *, unclassified protein selected from Table S2 in the supplemental material; **, predicted high-affinity glucose transporter (Table 3).

or as a precursor of γ-aminobutyrate, whose further metabolization is important for counteracting oxidative stress in *S. cerevisiae* and *Arabidopsis thaliana* (25, 31). The key enzyme of the γ-aminobutyrate shunt, γ-aminobutyrate transaminase, showed enhanced expression in the *ramosa-1* mutant (An17g00910 in Fig. 6), which could probably point toward increased ROS production in the *ramosa-1* mutant. Supportive of this assumption is upregulation of other *A. niger* genes which show considerable sequence homology to oxidative stress-responsive and ROS-scavenging proteins from other eukaryotes, e.g., D-arabinose dehydrogenase (An01g06970), platelet-activating factor acetylhydrolase (An09g01050), and manganese superoxide dismutase (An01g12530) (1, 58, 99).

Finally, 13 genes in the category related to metabolism with predicted function in cell wall biosynthesis and integrity were significantly upregulated in the *ramosa-1* mutant, whereas two genes were downregulated (Table 3 and Fig. 7), indicating that apical branching is accompanied by considerable cell wall reorganization. Congruently, the *mkkA* gene (An18g03740), encoding a MAP kinase kinase predicted to function in the CWI signaling pathway of *A. niger*, showed increased expression. To the group of upregulated cell wall genes belonged a chitin synthase gene (An07g05570), whose increased expression might explain the apparent enhanced chitin level in the *ramosa-1* mutant as shown in Fig. 4g.

Six genes predicted to function in the synthesis of (phospho)-lipid signaling molecules such as phosphatidate (PA) (An02g08050 and An15g07040; reactions 3 and 4 in Fig. 7), phosphatidylinositol-4′-monophosphate (PIP) (An18g06410, reaction 5 in Fig. 7), diacylglycerol (DAG) (An04g03870 and An11g05330, reactions 1 and 2 in Fig. 7), and inositolpyrophosphates (IP) (An16g05020, reaction 6 in Fig. 7) were upregulated in the *ramosa-1* mutant (Table 3 and Fig. 7). These molecules play important roles in the regulation of actin polarization, CWI, and calcium signaling in lower and higher eukaryotes (see Discussion and Fig. 7), thus probably reflecting an important influence of phospholipid signaling in the process of apical branching.

Furthermore, genes encoding putative effector proteins of the calcium signaling machinery were upregulated, such as two Ca^{2+}/calmodulin-dependent protein kinases (An02g05490 and An16g03050) and three vacuolar Ca^{2+} pumps (An02g06350, An01g03100, and An05g00170), hinting at the possibility that the mechanisms underlying apical branching might, beside CWI and phospholipid signaling, also involve the calcium signaling machinery (Fig. 7). In support of this notion is the most recent observation that a strong calcium spike accompanies apical branching in *Fusarium oxysporum* hyphae (54). Finally, 12 genes putatively encoding transport proteins for ions (P_i, Na^+, K^+, Fe^{2+}, and Zn^{2+}) and small molecules (phospholipids, amino acids, peptides, and glucose) displayed differential transcription in the *ramosa-1* mutant (Table 3), suggesting that (i) apical branching might in general require ion homeostatic and metabolic control systems and/or (ii) the RmsA protein has a function not only in actin polarization but additionally in ion homeostasis and energy metabolism.

Promoter analysis of differentially expressed genes. In order to unravel potential transcription factors involved in up- or downregulation of the 136 differentially expressed genes, we screened the 1,000-bp upstream regions of all genes for the presence of binding sites established for 25 transcription factors from different *Aspergillus* and *Trichoderma* species (using the in-house-developed TFBSF). We also used MEME (6) to screen for the presence of common but new DNA binding motifs. We determined the frequency of occurrence of these

TABLE 2. Functional categories of genes up- or downregulated in the *ramosa-1* mutant compared to wild-type strain T312[a]

Functional category	No. of genes:	
	Upregulated	Downregulated
Metabolism	32	11
Amino acid metabolism	4	1
Nitrogen and sulfur metabolism	2	1
Nucleotide metabolism	1	1
Phosphate metabolism	1	
C compound and carbohydrate metabolism	18	7
Lipid, fatty acid, and isoprenoid metabolism	6	1
Energy	2	
Cell cycle and DNA processing	2	1
Transcription	2	1
Protein synthesis		
Protein fate	7	
Cellular transport and transport mechanism	5	2
Cellular communication	1	
Cell rescue, defense, and virulence	3	
Regulation of/interaction with cellular environment	2	
Subcellular localization	2	1
Transport facilitation	1	1
Unclassified proteins	50	10

[a] An annotated list of all responsive genes, including the fold change, *P* value, and classification, can be found in Table S2 in the supplemental material. Statistically enriched FunCat subcategories, determined by using the gene set enrichment analysis tool (93) (false discovery rate, <0.05), are also depicted in Table S2 in the supplemental material.

TABLE 3. Selected responsive genes in the *ramosa-1* mutant, ordered into different processes and functions

Category and ORF	Gene[a]	Fold change[b]	*P* value	Predicted protein function[c]	Closest *S. cerevisiae* homolog
Energy generation					
An02g06820		2.62	0.024	Pyruvate decarboxylase	Pdc6
An02g02060		2.15	0.039	Alcohol dehydrogenase	
Amino acid metabolism					
An11g07960		(9.74)	0.025	Glutaminase	
An17g00910		6.03	0.004	γ-Aminobutyrate transaminase	Uga1
An02g14590		3.15	0.029	NAD^+-dependent glutamate dehydrogenase	Gdh2
Oxidative stress-responsive proteins					
An09g01050		(22.64)	0.038	PAFAH, removal of oxidized membrane phospholipids	
An15g07670		(10.66)	0.055	Tyrosinase involved in melanin synthesis	
An01g06970		6.506	0.005	D-Arabinose dehydrogenase	Ara1
An06g01610		(3.97)	0.029	Heat shock protein	Hsp12
An15g01840		2.49	0.038	Secoisolariciresinol dehydrogenase	
An01g12530		2.39	0.055	Manganese superoxide dismutase	Sod2
Cell wall synthesis and remodeling					
An16g06120	*gelF*	(78.40)	0.004	Glycosylphosphatidylinositol-anchored β-1,3-glucanosyltransferase	Gas1
An04g03830		18.18	0.006	Glycosylphosphatidylinositol-anchored cell wall protein	
An13g02510	*crhE*	7.49	0.003	Glycosylphosphatidylinositol-anchored chitin transglycosidase	Crh1
An11g06540	*mndA*	(4.24)	0.033	β-Mannosidase	
An03g05560		3.74	0.008	Spherulin 4-like cell surface protein	
An18g03740	*mkkA*	3.72	0.025	MAP kinase kinase involved in CWI pathway	Mkk1/2
An16g08090	*dfgE*	3.24	0.043	Glycosylphosphatidylinositol-anchored endo-mannanase	Dfg1
An08g09610	*agnD*	3.17	0.016	α-1,3-Glucanase	
An07g05570	*chsA*	2.39	0.034	Chitin synthase class II, similar to ChsA of *A. nidulans*	Chs1
An14g03910		2.26	0.052	α-1,2-Mannosyltransferase	Kre2
An18g05910		(2.25)	0.041	α-1,2-Mannosyltransferase	Kre2
An03g05530		2.18	0.051	Endo-β-1,4-glucanase	
An04g05550		2.61	0.037	Mucin-like protein	Flo11
An02g11620		0.32	0.039	Cell wall protein	
An09g06400	*ctcA*	0.14	0.013	Glycosylphosphatidylinositol-anchored chitinase, similar to ChiA of *A. nidulans*	Cts1
Phospholipid signaling[d]					
An02g08050[3]		(12.36)	0.056	Phosphatidyl synthase, synthesis of phosphatidyl alcohols	
An01g07000		10.75	0.051	C_{14} sterol reductase, ergosterol synthesis	Erg24
An16g05020[6]		7.34	0.002	Inositol hexaki-/heptaki-phosphate kinase, synthesis of IP6/IP7	Vip1
An18g06410[5]		4.11	0.011	Plasma membrane protein promoting PI4P synthesis	Sfk1
An15g07040[4]		3.77	0.026	Phospholipase D, synthesis of PA	Spo14
An04g03870[2]		(3.24)	0.018	PA phosphatase, synthesis of DAG	
An11g05330[1]		1.95	0.051	Diacylglycerol pyrophosphate phosphatase, synthesis of DAG	Dpp1
Calcium signaling and homeostasis					
An02g05490		2.97	0.028	Ca^{2+}/calmodulin-dependent protein kinase	Cmk2
An16g03050		2.39	0.033	Ca^{2+}/calmodulin-dependent protein kinase	Cmk2
An02g06350		(5.48)	0.025	Vacuolar Ca^{2+}/H^+ exchanger	Pmc1
An01g03100		4.49	0.009	Vacuolar Ca^{2+}/H^+ exchanger	Vcx1
An05g00170		2.15	0.054	Vacuolar Ca^{2+}/H^+ exchanger	Vcx1
Other signaling processes					
An15g01560		(3.21)	0.029	GTPase-activating protein involved in protein trafficking	Gyp7
An04g01500		2.98	0.044	Putative C_2H_2 zinc finger transcription factor	
An08g07090		0.06	0.054	SUN family protein involved in replication	Sim1
An16g07890		0.04	0.037	Similar to *A. nidulans* transcription factor RosA	Ume6
An12g04710		0.29	0.031	Negative regulator of Cdc42	Vtc1
Transporters					
An02g04160		4.85	0.010	Mitochondrial phosphate translocator	Mir1
An13g02320		(4.70)	0.027	Vacuolar glutathione S-conjugate ABC transporter	Ycf1
An09g00930		3.44	0.055	Na^+/K^+-exchanging ATPase alpha-1 chain	
An02g01480		3.78	0.021	MFS multidrug transporter	
An16g06300		3.18	0.013	Low-affinity Fe(II) transporter	Fet4
An04g06840		2.39	0.052	Ca^{2+}/phospholipid-transporting ATPase	Drs2
An14g01860		0.41	0.051	Mitochondrial carrier protein	Rim2
An12g05510		0.38	0.024	Siderophore-iron transporter	Taf1
An15g03900		0.32	0.049	Vacuolar zinc transporter	Zrc1
An18g01220		0.29	0.059	Allantoin permease	Dal5
An15g07460		0.26	0.023	Oligopeptide transporter	
An09g04810		0.06	0.011	High-affinity glucose transporter	

[a] Proposed protein abbreviations according to reference 73.
[b] Parentheses indicate that the gene has an "Absent" flag in the control experiment.
[c] PAFAH, platelet-activating factor acetylhydrolase; MFS, major facilitator superfamily.
[d] Superscript numbers refer to reactions indicated in Fig. 7.

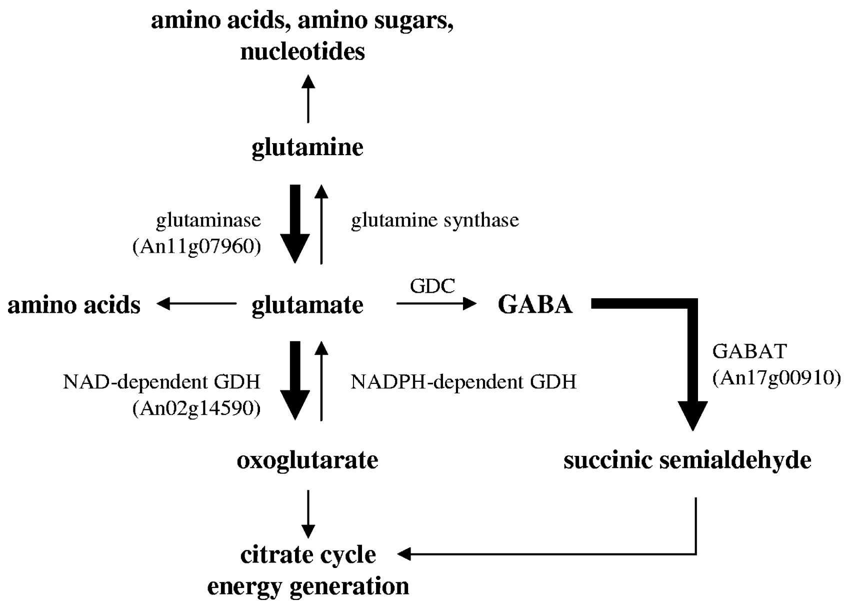

FIG. 6. Pathways involved in glutamate metabolism. Genes upregulated in the *ramosa-1* mutant are indicated with their ORF codes. The directions of the respective enzymatic reactions are indicated with thick arrows. GDH, glutamate dehydrogenase; GDC, glutamate decarboxylase; GABA, γ-aminobutyrate; GABAT, γ-aminobutyrate transaminase.

motifs in the group of 109 upregulated and 27 downregulated genes and evaluated whether these motifs are statistically significant over- or underrepresented compared to groups of the same size comprising randomly selected genes of *A. niger* (500,000 bootstrap samples, $P < 0.05$).

Using these in silico approaches, we were able to identify four motifs with the TFBSF tool and 27 motifs with the MEME tool as being enriched or underrepresented within the upstream regions of genes upregulated in the *ramosa-1* mutant. As shown in detail in Table S3 in the supplemental material, the four enriched *Aspergillus* motifs identified with the TFBSF tool were also among the sites identified by MEME and are binding motifs of the transcription factors AbaA (asexual development and dimorphism) (2, 17, 57), CrzA (calcium signaling, cell wall formation, and polar growth) (33, 91), CreA (carbon catabolite repression and polar growth) (59, 112), and AmdR (amino acid utilization) (27), respectively. Among the set of MEME sites, we could additionally identify one site as a BrlA site (asexual development) (23) and three sites as cyclic AMP-responsive elements involved in protein kinase A signaling (metabolism, polar growth, and dimorphism) (11, 16, 38). Within the set of genes downregulated in the *ramosa-1* mutant, three overrepresented sites were identified with the TFBSF tool which were also present among the 10 identified MEME sites (see Table S3 in the supplemental material): Seb1 (osmotic stress response) (74), AnCP/AnCF (CCAAT binding factor involved in, e.g., respiration) (21, 53), and BrlA (asexual development) (23). These data are in good agreement with the microarray and phenotypic data obtained which suggested a complex reorganization in the *ramosa-1* mutant involving polar growth control, carbon and nitrogen metabolism, respiration, and calcium homeostasis.

For the majority of the known *Aspergillus*/*Trichoderma* transcription factor binding sites analyzed (15), we found a similar frequency of occurrence in genes differentially expressed in the *ramosa-1* mutant compared to randomly selected genes (see Table S3 in the supplemental material). Although this does not necessarily preclude these *trans* factors from any role in the *ramosa-1* mutant transcriptional response, it can be speculated that their involvement in regulating early events during apical branching is less important than the involvement of transcription factors showing enriched or underrepresented motifs. To our surprise, however, binding sites for the effector regulator of the CWI pathway RlmA are not significantly overrepresented in genes upregulated in the *ramosa-1* mutant, suggesting that (i) RlmA does not have the same prominent function as its *S. cerevisiae* ortholog Rlm1p (i.e., not all *A. niger* cell wall-related genes are regulated by RlmA), (ii) CWI activates not only RlmA but also another as-yet-unknown transcription factor(s), or (iii) CWI signaling is not the only pathway responsible for the expression of cell wall-related genes.

DISCUSSION

The *ramosa-1* mutant as a model system to study polarity control. This study shows that the *ramosa-1* strain can be considered an excellent model system to study the morphogenetic program of *A. niger*. All critical steps of hyphal morphogenesis (establishment, maintenance, and loss of maintenance of polar axes) can be altered within a single system by changing the cultivation temperature. Hence, different aspects of fungal polarity can be simultaneously studied in this strain. In addition, this model system can be used to address the question of whether an increase in the number of branches (per total cell mass) will indeed improve protein secretion in *A. niger*. Using the approach described in this study, the frequency of branching as well as the length of hyphal compartments can easily be adjusted by running defined temperature programs. Determi-

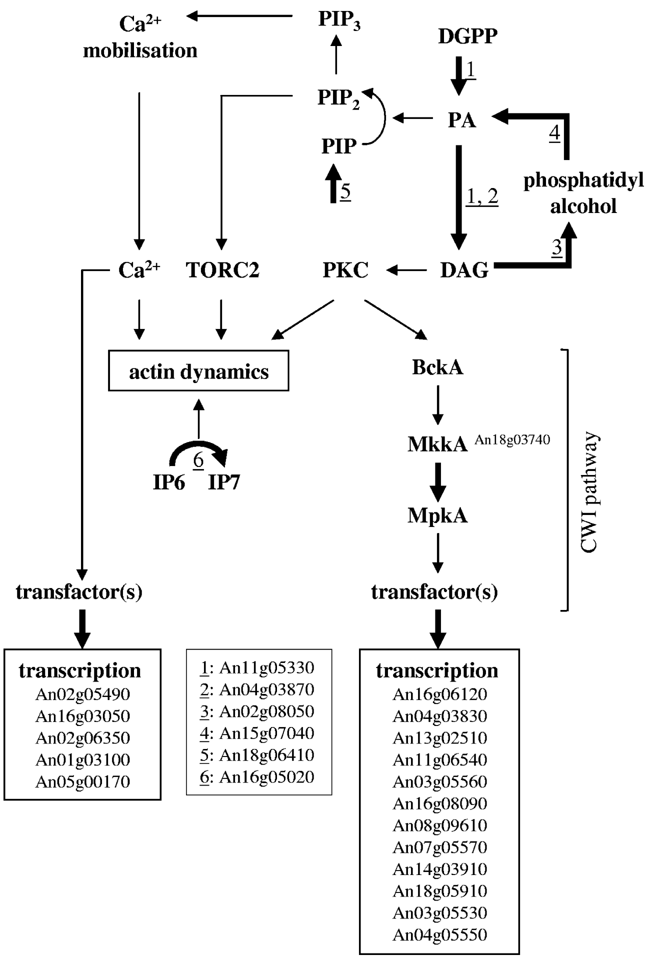

FIG. 7. Genes upregulated in the *ramosa-1* mutant and their allocation into the processes of cell wall synthesis, (phospho)lipid synthesis, and calcium homeostasis (indicated with thick arrows). For the predicted gene functions, see Table 3. For explanations of the connection of these processes in eukaryotes, see Discussion.

nation of the amount of secreted proteins and its relation to the amount of branches per hyphal compartment can be one systematic attempt to answer this question. Furthermore, the *ramosa-1* mutant offers the possibility to determine the optimal number of branches per hyphal compartment in order to improve the rheological behavior of *A. niger* in industrial settings.

A proposed role for RmsA in polarity control. Only a single point mutation within the *rmsA* gene is responsible for the mutant phenotype of the *ramosa-1* mutant. The Y447N mutation of RmsA seems to have no apparent consequence for the growth of the *ramosa-1* mutant when it is cultivated at low temperature (24°C), suggesting that $RmsA^{Y447N}$ can still fulfill its cellular function. However, at higher temperature, Y447 seems to be essential for the function of RmsA, and its change to asparagine has profound consequences on the growth of *A. niger*, such as loss of polarity maintenance, slow growth, and defective asexual development (this work and reference 77). Several scenarios are imaginable to explain this temperature-dependent phenotype: (i) $RmsA^{Y447N}$ is stable but lowered in its stability at 37°C and becomes readily degraded, (ii) an interaction of $RmsA^{Y447N}$ with other proteins is possible at low temperature but disturbed at higher temperature, or (iii) RmsA is crucial for the survival of *A. niger* at high but not at low temperature. Our data seem to exclude the third possibility, as deletion of the *rmsA* gene is already lethal for *A. niger* when it is cultivated at 25°C.

The lethality of *AVO1* deletion in *S. cerevisiae* can be complemented by *rmsA*, demonstrating that RmsA is a functional equivalent of Avo1p, a component of the *S. cerevisiae* TORC2 complex (61). Avo1p is essential for the maintenance of TORC2 integrity (109), a complex that is composed of six proteins, namely Avo1p, Avo2p, Avo3p/Tsc11p, Lst8p, Bit61p, and Tor2p (30, 61, 76). With the exception of Avo2p and Bit61p, sequences with obvious similarity to all *S. cerevisiae* TORC2 components can be found in the genome of *A. niger* (see Table S4 in the supplemental material). Respective sequences (except for Avo2p and Bit61p, which appear to be unique to *S. cerevisiae*) are also present in other eukaryotes ranging from *S. pombe* over *Drosophila* to mammals and have at least partially been shown to associate in a TORC2 complex (109). This high degree of evolutionary conservation makes it reasonable to predict that a TORC2-like complex exists in *A. niger* and that RmsA is a component of it.

TORC2 has an essential function for actin polarization and hence determination of cell polarity in *S. cerevisiae*, *Dictyostelium discoideum*, and mammalian cells but not in the fission yeast *S. pombe* (63, 109). In this study, we have observed a depolarized actin localization at the hyphal tip when the *ramosa-1* mutant is cultivated at the restrictive temperature (Fig. 4), strongly suggesting that RmsA, i.e., the proposed *A. niger* TORC2, carries out a function in cytoskeletal organization. Most interestingly, the disturbed actin localization observed is reminiscent of the subapical localization of actin in the *act[1]* mutant of *N. crassa*, a mutant that displays increased apical branching (101). Loss of actin polarization in the *ramosa-1* mutant (hypothetically due to reduced TORC2 integrity as a consequence of a less functional $RmsA^{Y447N}$) may thus be considered as a key event of apical branching.

Transcriptomic insights into the process of apical branching. What, then, are the cellular events involved in apical branching? The transcriptomic data obtained in this work are most probably a reflection of two events: (i) the consequences of a defective RmsA/TORC2 function(s) (resulting in loss of polarity and disturbance of other TORC2-controlled processes) and (ii) establishment of two new polarity axes. The function of TORC2 in polar growth control via regulation of actin polarization and/or protein kinase C (PKC) activities is conserved from yeast to mammals (reviewed in reference 49). Additionally, TORC2 has also been reported to be an upstream regulator of another TOR-containing complex (TORC1) in mammals (49). TORC1 is also conserved from yeast to mammals and regulates a myriad of cell growth-related processes (e.g., transcription, translation, and protein turnover) by integrating signals from nutrients, energy status, and stressors. Thus, TORC1 regulates temporal growth, whereas TORC2 regulates spatial growth (49). However, the discovery that mammalian TORC2 acts not only in parallel to but also upstream of TORC1 brings challenge in understanding TORC2 signaling mechanisms and in answering the question posed above. The transcriptomic response of the *ramosa-1* mutant includes changes in carbon, nitrogen, (phospho)lipid, and energy metabolism as well as in the stress response and ion homeostasis. As mentioned above, probably not all of these responses are related to the process of apical branching. Below, we propose and discuss a possible involvement of three cellular processes in the process of apical branching—(phospho)lipid signaling, calcium signaling, and CWI signaling—and their suspected connections to TORC2 functions.

The synthesis of important (phosho)lipid signaling molecules (PA, DAG, and PIP) and IP seems to be increased during apical branching, as genes encoding the corresponding synthetic enzymes showed enhanced expression (Table 3 and Fig. 7). Although the function of PA has not been studied in detail for filamentous fungi, a recent report demonstrated that reduced production of PA causes polarity defects in *A. nidulans* (62), which supports our data. Importantly, PA serves as precursor for DAG in *S. cerevisiae*, which in turn functions as activator of PKC (Pkc1p), a component of the CWI pathway which is localized upstream of the MAP kinase kinase Mkk1/2p (MkkA) (Fig. 7) (for a review, see reference 103). PA, however, has multiple regulatory roles in eukaryotes, such as promotion of actin polymerization and activation of TOR and PI(4)5 kinases to increase conversion from PIP to phosphatidylinositol-4′,5′-bisphosphate (PIP_2) (103). PIP_2 in turn can stimulate actin polymerization via interaction with actin-interacting proteins (reviewed in reference 24) and promotes actin remodeling by recruiting TORC2-interacting proteins (Slm1p and Slm2p) and different GTPases (e.g., Rho1p and its activator Rom2p) to membrane compartments (3, 4, 83). The GTPase Cdc42 has also been reported to activate mammalian PI(4)5 kinases, thereby increasing local PIP_2 levels (reviewed in reference 83). Interestingly, we found a downregulation of An12g04710, which displays similarity to the yeast Vtc1p and Nrf1p proteins, which are negative regulators of Cdc42 (70). Reduced expression of An12g04710 could thus also hint at increased PIP_2 synthesis during apical branching. Finally, An16g05020, a gene with homology to the genes encoding the *S. cerevisiae* Vip1p and *S. pombe* Asp1p proteins (inositol hexaki-/heptaki-phosphate kinase; reaction 6 in Fig. 7), showed increased expression. Asp1p has been reported to be necessary for the integrity of cortical actin patch organization (32).

Remarkably, PIP_2 serves as precursor for phosphatidylinositol-1′,4′,5′-triphosphate (PIP_3), which has been described as inducing calcium release from intracellular stores in mammalian cells (reviewed in reference 7). An increase in cytosolic calcium levels has been shown to activate the calcium/calmodulin/calcineurin/Crz1p signaling pathway in *S. cerevisiae*, which induces calcineurin- or Crz1p-dependent transcription of genes whose protein products are involved in ion homeostasis, cell wall synthesis, and signaling (reviewed in reference 26). All components of this pathway are conserved in *A. niger* (see Table S5 in the supplemental material). CrzA, the *A. nidulans* homolog of Crz1p, has also been demonstrated to be positively involved in transcriptional regulation of a chitin synthase gene (*chsB*) and the *vcxA* gene, encoding a vacuolar Ca^{2+} pump (91). Among the genes upregulated in the *ramosa-1* mutant, at least five genes whose protein products can be predicted to function in calcium signaling and homeostasis were identified, i.e., two Ca^{2+}/calmodulin-dependent protein kinases and three vacuolar Ca^{2+} pumps (two of these encode *VCX1*/*vcxA*-homologous genes). However, other *A. niger* genes also might be effector genes of a calcium response, as CrzA binding motifs were significantly overrepresented in genes upregulated in the *ramosa-1* mutant (see Table S3 in the supplemental material). Furthermore, a recent finding in *S. cerevisiae* demonstrated that calcineurin negatively controls TORC2 and that TORC2 negatively regulates calcineurin, a mutual antagonism that is also reflected by the observation that about 50% of the genes which are upregulated during TORC2 inhibition overlap with calcineurin/Crz1p-dependent genes (69). Among this set of overlapping *S. cerevisiae* genes are also genes showing increased expression in the *ramosa-1* mutant (An15g01560/GTPase Gyp7p, An02g06350/vacuolar Ca^{2+}/H^{+} exchanger Pmc1p, An02g05490 and An16g03050/protein kinase Cmk2, and An00g07168/aspartic protease) (Table 3; see Table S2 in the supplemental material). Most importantly, this report has evidenced that calcineurin-mediated events cause depolarization of the actin cytoskeleton, whereas TORC2 counteracts this process—opposing control mechanisms that have also been observed in mammalian cells (see reference 69 and references therein). The *ramosa-1* transcriptome data hint at the possibility that a similar antagonism might occur in *A. niger*; i.e., actin depolarization in the *ramosa-1* mutant might be a consequence of increased calcium signaling which originates from defective TORC2 signaling.

The actin organization defect in an *S. cerevisiae* conditional *tor2* loss-of-function mutant (*tor2^ts^*) can be suppressed by overexpressing CWI pathway components (for a review, see reference 60). Our data demonstrated enhanced transcription of the predicted CWI component *mkkA*, point toward activation of PkcA by DAG, showed increased expression of cell wall biosynthesis and remodeling genes, and suggested increased chitin deposition in the *ramosa-1* mutant (Fig. 4 and Table 3). These responses resemble the connection between TORC2 and CWI signaling in *S. cerevisiae*, suggesting that reinforced CWI signaling in the *ramosa-1* mutant could be an adaptive response to counteract defective $RmsA^{Y447N}$ (i.e., TORC2) function.

Finally, the transcriptomic data also point toward increased expression of oxidative stress response genes in the *ramosa-1* mutant (Table 3). However, the fact that we could not detect any differences in tip-localized ROS staining in *ramosa-1* and wild-type germlings (Fig. 4) suggests that increased ROS production can be sufficiently counteracted by enhanced expression of ROS-scavenging genes in the *ramosa-1* mutant. An appealing explanation for the observed induction of oxidative stress genes might be given by a recent report on *S. cerevisiae*, where it has been demonstrated that TORC2 inhibits the response to oxidative stress (69). In other words, defective TORC2 signaling in the *ramosa-1* mutant could mimic the presence of oxidative stress within the cell and might further reflect a similar interconnection between TORC2, oxidative stress, CWI, and calcium signaling pathways in *A. niger* as reported for *S. cerevisiae*. Taken together, the transcriptomic fingerprint of the *ramosa-1* mutant suggests that at least four signaling cascades might be involved in the process of apical branching: (phospho)lipid, calcium, TORC2, and CWI signaling. In our previous work, we used a pharmacological approach to induce (sub)apical branch formation in *A. niger* germlings. The transcriptomic profiles obtained likewise suggested a role

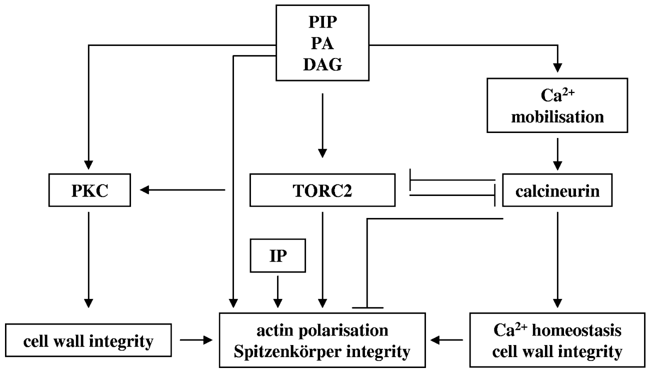

FIG. 8. A reconstructed model for polarity control and apical branching in *A. niger*. The model rests on transcriptomic and phenotypic data obtained from *ramosa-1* mutant and wild-type *A. niger* (this work and references 77 and 78), as well as on assumptions deduced from conserved mechanisms in yeast and mammalian systems (see Discussion for references). Basically, TORC2 exerts at least three important cellular functions. (i) TORC2 plays a crucial role in maintaining actin polarization, among other things, via calcineurin inhibition. (ii) TORC2 is essential for cell wall biosynthesis and activates PKC, the initiator kinase of the CWI pathway. (iii) TORC2 inhibits expression of oxidative stress genes under nonstressed conditions (not indicated in the figure). RmsA^{Y447N}, however, negatively interferes with *A. niger* TORC2 function, resulting in actin depolarization, induction of apical branch formation, and derepression of oxidative stress genes. To counteract failure of TORC2, increased synthesis of important (phospho)lipid signaling molecules takes place (reactions 1 to 6) (Table 3 and Fig. 7), resulting in (i) increased Rom2p/Rho1p activation (via PIP_2) aiming to repolarize actin, (ii) reactivation of TORC2 (via PIP_2), (iii) reinforced PKC activation (via DAG) and thereby amplified expression of cell wall-related genes, and (iv) repolarization of actin (via IP7).

for (phospho)lipid, TORC2, and CWI signaling during polarity control (67).

A hypothetic model for cellular events involved in apical branching. We previously proposed "that the apical branching phenotype in *ramosa-1* is triggered by a molecular event that induces a transient alteration in cytoskeleton organization" (77, 78). Our present transcriptomic analysis shows a number of changes that either singly or in combination would bring about the physiological changes that contract the actin cytoskeleton, dislodge the Spitzenkörper, interrupt hyphal elongation, and set the stage for the subsequent formation of two new centers of polarized growth. Based upon transcriptomic, genetic, and phenotypic data obtained in this study and in our previous work (77, 78), we propose the following working model for the process of apical branching in *A. niger* (Fig. 8). We hypothesize that the actin polarization defect in the *ramosa-1* mutant is evoked by a nonfunctional or partially functional RmsA^{Y447N} protein, whereas in wild-type cells, the primary trigger for a momentary disruption of actin integrity has yet to be identified. As a consequence of actin depolarization, the Spitzenkörper detaches from the apex and disintegrates, and polarity maintenance becomes lost in the leading hypha. This event is counteracted by increased (phospho)lipid and CWI signaling aiming at actin repolarization and increased cell wall biosynthesis, whereupon two new Spitzenkörper and thereby two new polarity axes become established. The stability of these polarity axes, however, cannot be maintained in the *ramosa-1* mutant: increased (phospho)lipid signaling provokes excessive calcium release from internal stores, which results in enhanced calcineurin activity, the hypothetic cause for redepolarization of actin. In wild-type hyphae, however, intact TORC2 signaling antagonizes calcineurin-mediated actin depolarization, thereby ensuring polarity maintenance.

Conclusions. This work provides the first molecular insights into the nature of apical branching of *A. niger* and potential RmsA function. The genes belonging to the transcriptomic fingerprint of apical branching constitute a valuable compilation of genes, whose further analysis will unravel their exact contribution to polar growth of *A. niger*. The apical branching transcriptome of the *ramosa-1* mutant allowed us to reconstruct and predict mechanistic details of signaling networks putatively involved in polarity control in *A. niger*. The exact functions of the presumed networks as well as their interconnections remain to be elucidated in future studies, as do the identities of the *A. niger* TORC2 complex and its targets.

ACKNOWLEDGMENTS

We acknowledge Peter Punt and Frank Schuren for providing us with the *A. niger* cosmid and cDNA libraries. We thank the anonymous reviewers for their helpful suggestions to improve the manuscript.

The research group of C.A.M.J.J.v.d.H. is part of the Kluyver Centre for Genomics of Industrial Fermentation, which is supported by The Netherlands Genomics Initiative.

REFERENCES

1. **Amako, K., K. Fujita, C. Iwamoto, M. Sengee, K. Fuchigami, J. Fukumoto, Y. Ogishi, R. Kishimoto, and K. Goda.** 2006. NADP(+)-dependent D-arabinose dehydrogenase shows a limited contribution to erythroascorbic acid biosynthesis and oxidative stress resistance in *Saccharomyces cerevisiae*. Biosci. Biotechnol. Biochem. **70:**3004–3012.
2. **Andrianopoulos, A., and W. E. Timberlake.** 1994. The *Aspergillus nidulans abaA* gene encodes a transcriptional activator that acts as a genetic switch to control development. Mol. Cell. Biol. **14:**2503–2515.
3. **Audhya, A., and S. D. Emr.** 2002. Stt4 PI 4-kinase localizes to the plasma membrane and functions in the Pkc1-mediated MAP kinase cascade. Dev. Cell **2:**593–605.
4. **Audhya, A., R. Loewith, A. Parsons, L. Gao, M. Tabuchi, H. Zhou, C. Boone, M. Hall, and S. Emr.** 2004. Genome-wide lethality screen identifies new PI4,5P2 effectors that regulate the actin cytoskeleton. EMBO J. **23:** 3747–3757.
5. **Ayad-Durieux, Y., P. Knechtle, S. Goff, F. Dietrich, and P. Philippsen.** 2000. A PAK-like protein kinase is required for maturation of young hyphae and septation in the filamentous ascomycete *Ashbya gossypii*. J. Cell Sci. **113:** 4563–4575.
6. **Bailey, T. L., and C. Elkan.** 1994. Fitting a mixture model by expectation maximization to discover motifs in biopolymers. Proc. Int. Conf. Intell. Syst. Mol. Biol. **2:**28–36.
7. **Balla, T.** 2006. Phosphoinositide-derived messengers in endocrine signaling. J. Endocrinol. **188:**135–153.
8. **Bartnicki-García, S.** 2002. Molecular biology of fungal development, p. 29–58. Marcel Decker Inc., New York, NY.
9. **Bartnicki-García, S.** 2006. Chitosomes: past, present and future. FEMS Yeast Res. **6:**957–965.
10. **Bartnicki-García, S., F. Hergert, and G. Gierz.** 1989. Computer simulation of fungal morphogenesis and the mathematical basis for hyphal tip growth. Protoplasma **153:**46–57.
11. **Bencina, M., M. Legisa, and N. D. Read.** 2005. Cross-talk between cAMP and calcium signalling in *Aspergillus niger*. Mol. Microbiol. **56:**268–281.
12. **Benjamini, Y., and Y. Hochberg.** 1995. Controlling the false discovery rate: a practical and powerful approach to multiple testing. J. R. Stat. Soc. Ser. B **57:**289–300.
13. **Bennett, J. W., and L. Lasure.** 1991. More gene manipulations in fungi. Academic Press, San Diego, CA.
14. **Bocking, S. P., M. G. Wiebe, G. D. Robson, K. Hansen, L. H. Christiansen, and A. P. Trinci.** 1999. Effect of branch frequency in *Aspergillus oryzae* on protein secretion and culture viscosity. Biotechnol. Bioeng. **65:**638–648.
15. **Bok, J. W., T. Sone, L. B. Silverman-Gavrila, R. R. Lew, F. J. Bowring, D. E. Catcheside, and A. J. Griffiths.** 2001. Structure and function analysis of the calcium-related gene spray in *Neurospora crassa*. Fungal Genet. Biol. **32:** 145–158.

16. **Borges-Walmsley, M. I., and A. R. Walmsley.** 2000. cAMP signalling in pathogenic fungi: control of dimorphic switching and pathogenicity. Trends Microbiol. **8:**133–141.
17. **Borneman, A. R., M. J. Hynes, and A. Andrianopoulos.** 2000. The *abaA* homologue of Penicillium marneffei participates in two developmental programmes: conidiation and dimorphic growth. Mol. Microbiol. **38:**1034–1047.
18. **Borsuk, P., M. Nagieć, P. Stepień, and E. Bartnik.** 1982. Organization of the ribosomal RNA gene cluster in *Aspergillus nidulans*. Gene **17:**147–152.
19. **Bourett, T. M., and R. J. Howard.** 1991. Ultrastructural immunolocalisation of actin in a fungus. Protoplasma **163:**199–202.
20. **Bracker, C. E., J. Ruiz-Herrera, and S. Bartnicki-Garcia.** 1976. Structure and transformation of chitin synthetase particles (chitosomes) during microfibril synthesis in vitro. Proc. Natl. Acad. Sci. USA **73:**4570–4574.
21. **Brakhage, A. A., A. Andrianopoulos, M. Kato, S. Steidl, M. A. Davis, N. Tsukagoshi, and M. J. Hynes.** 1999. HAP-like CCAAT-binding complexes in filamentous fungi: implications for biotechnology. Fungal Genet. Biol. **27:**243–252.
22. **Carol, R. J., and L. Dolan.** 2006. The role of reactive oxygen species in cell growth: lessons from root hairs. J. Exp. Bot. **57:**1829–1834.
23. **Chang, Y. C., and W. E. Timberlake.** 1993. Identification of *Aspergillus brlA* response elements (BREs) by genetic selection in yeast. Genetics **133:**29–38.
24. **Chen, H., B. W. Bernstein, and J. R. Bamburg.** 2000. Regulating actin-filament dynamics in vivo. Trends Biochem. Sci. **25:**19–23.
25. **Coleman, S., T. Fang, S. Rovinsky, F. Turano, and W. Moye-Rowley.** 2001. Expression of a glutamate decarboxylase homologue is required for normal oxidative stress tolerance in *Saccharomyces cerevisiae*. J. Biol. Chem. **276:**244–250.
26. **Cyert, M. S.** 2003. Calcineurin signaling in *Saccharomyces cerevisiae*: how yeast go crazy in response to stress. Biochem. Biophys. Res. Commun. **311:**1143–1150.
27. **Davis, M. A., J. M. Kelly, and M. J. Hynes.** 1993. Fungal catabolic gene regulation: molecular genetic analysis of the *amdS* gene of *Aspergillus nidulans*. Genetica **90:**133–145.
28. **deHart, A., J. Schnell, D. Allen, J. Tsai, and L. Hicke.** 2003. Receptor internalization in yeast requires the Tor2-Rho1 signaling pathway. Mol. Biol. Cell **14:**4676–4684.
29. **de Ruiter-Jacobs, Y. M., M. Broekhuijsen, S. E. Unkles, E. I. Campbell, J. R. Kinghorn, R. Contreras, P. H. Pouwels, and C. A. van den Hondel.** 1989. A gene transfer system based on the homologous *pyrG* gene and efficient expression of bacterial genes in *Aspergillus oryzae*. Curr. Genet. **16:**159–163.
30. **Fadri, M., A. Daquinag, S. Wang, T. Xue, and J. Kunz.** 2005. The pleckstrin homology domain proteins Slm1 and Slm2 are required for actin cytoskeleton organization in yeast and bind phosphatidylinositol-4,5-bisphosphate and TORC2. Mol. Biol. Cell **16:**1883–1900.
31. **Fait, A., A. Yellin, and H. Fromm.** 2005. GABA shunt deficiencies and accumulation of reactive oxygen intermediates: insight from *Arabidopsis* mutants. FEBS Lett. **579:**415–420.
32. **Feoktistova, A., D. McCollum, R. Ohi, and K. Gould.** 1999. Identification and characterization of *Schizosaccharomyces pombe asp1*(+), a gene that interacts with mutations in the Arp2/3 complex and actin. Genetics **152:**895–908.
33. **Fortwendel, J. R., P. R. Juvvadi, N. Pinchai, B. Z. Perfect, J. A. Alspaugh, J. R. Perfect, and W. J. Steinbach.** 2009. Differential effects of inhibiting chitin and 1,3-β-D-glucan synthesis in Ras and calcineurin mutants of *Aspergillus fumigatus*. Antimicrob. Agents Chemother. **53:**476–482.
34. **Geitmann, A., and A. M. Emons.** 2000. The cytoskeleton in plant and fungal cell tip growth. J. Microsc. **198:**218–245.
35. **Girbardt, M.** 1957. Der Spitzenkörper von Polystictus versicolor. Planta **50:**47–59.
36. **Gordon, C. L., V. Khalaj, A. F. Ram, D. B. Archer, J. L. Brookman, A. P. Trinci, D. J. Jeenes, J. H. Doonan, B. Wells, P. J. Punt, C. A. van den Hondel, and G. D. Robson.** 2000. Glucoamylase::green fluorescent protein fusions to monitor protein secretion in *Aspergillus niger*. Microbiology **146:**415–426.
37. **Grimm, L. H., S. Kelly, R. Krull, and D. C. Hempel.** 2005. Morphology and productivity of filamentous fungi. Appl. Microbiol. Biotechnol. **69:**375–384.
38. **Grosse, C., T. Heinekamp, O. Kniemeyer, A. Gehrke, and A. A. Brakhage.** 2008. Protein kinase A regulates growth, sporulation, and pigment formation in *Aspergillus fumigatus*. Appl. Environ. Microbiol. **74:**4923–4933.
39. **Grove, S. N., and C. E. Bracker.** 1970. Protoplasmic organization of hyphal tips among fungi: vesicles and Spitzenkörper. J. Bacteriol. **104:**989–1009.
40. **Guthrie, C., and G. R. Fink (ed.).** 1991. Guide to yeast genetics and molecular biology. Methods Enzymol. **194:**1–933.
41. **Harris, S., J. Morrell, and J. Hamer.** 1994. Identification and characterization of *Aspergillus nidulans* mutants defective in cytokinesis. Genetics **136:**517–532.
42. **Harris, S. D.** 2008. Branching of fungal hyphae: regulation, mechanisms and comparison with other branching systems. Mycologia **100:**823–832.
43. **Harris, S. D., and M. Momany.** 2004. Polarity in filamentous fungi: moving beyond the yeast paradigm. Fungal Genet. Biol. **41:**391–400.
44. **Harris, S. D., N. D. Read, R. W. Roberson, B. Shaw, S. Seiler, M. Plamann, and M. Momany.** 2005. Polarisome meets Spitzenkörper: microscopy, genetics, and genomics converge. Eukaryot. Cell **4:**225–229.
45. **Howard, R. J.** 1981. Ultrastructural analysis of hyphal tip cell growth in fungi: Spitzenkörper, cytoskeleton and endomembranes after freeze-substitution. J. Cell Sci. **48:**89–103.
46. **Ikeda, K., S. Morigasaki, H. Tatebe, F. Tamanoi, and K. Shiozaki.** 2008. Fission yeast TOR complex 2 activates the AGC-family Gad8 kinase essential for stress resistance and cell cycle control. Cell Cycle **7:**358–364.
47. **Inoki, K., and K. L. Guan.** 2006. Complexity of the TOR signaling network. Trends Cell Biol. **16:**206–212.
48. **Irizarry, R. A., B. M. Bolstad, F. Collin, L. M. Cope, B. Hobbs, and T. P. Speed.** 2003. Summaries of Affymetrix GeneChip probe level data. Nucleic Acids Res. **31:**e15.
49. **Jacinto, E., and A. Lorberg.** 2008. TOR regulation of AGC kinases in yeast and mammals. Biochem. J. **410:**19–37.
50. **Jones, K. T., E. R. Greer, D. Pearce, and K. Ashrafi.** 2009. Rictor/TORC2 regulates *Caenorhabditis elegans* fat storage, body size, and development through sgk-1. PLoS Biol. **7:**e60.
51. **Jones, M., M. Raymond, Z. Yang, and N. Smirnoff.** 2007. NADPH oxidase-dependent reactive oxygen species formation required for root hair growth depends on ROP GTPase. J. Exp. Bot. **58:**1261–1270.
52. **Kasuga, T., and N. L. Glass.** 2008. Dissecting colony development of *Neurospora crassa* using mRNA profiling and comparative genomics approaches. Eukaryot. Cell **7:**1549–1564.
53. **Kato, M., A. Aoyama, F. Naruse, Y. Tateyama, K. Hayashi, M. Miyazaki, P. Papagiannopoulos, M. A. Davis, M. J. Hynes, T. Kobayashi, and N. Tsukagoshi.** 1998. The *Aspergillus nidulans* CCAAT-binding factor AnCP/AnCF is a heteromeric protein analogous to the HAP complex of *Saccharomyces cerevisiae*. Mol. Gen. Genet. **257:**404–411.
54. **Kim, H. S., K. Czymmek, and S. Kang.** 2009. Development of fluorescent protein-based biosensors for Ca^{2+} and pH to monitor physiological changes during *Arabidopsis thaliana-Fusarium oxysporum* interactions. Abstr. 25th Fungal Genetics Conference, p. 559.
55. **Knechtle, P., F. Dietrich, and P. Philippsen.** 2003. Maximal polar growth potential depends on the polarisome component AgSpa2 in the filamentous fungus *Ashbya gossypii*. Mol. Biol. Cell **14:**4140–4154.
56. **Knechtle, P., A. Kaufmann, D. Cavicchioli, and P. Philippsen.** 2008. The Paxillin-like protein AgPxl1 is required for apical branching and maximal hyphal growth in *A. gossypii*. Fungal Genet. Biol. **45:**829–838.
57. **Kohler, T., S. Wesche, N. Taheri, G. H. Braus, and H. U. Mosch.** 2002. Dual role of the *Saccharomyces cerevisiae* TEA/ATTS family transcription factor Tec1p in regulation of gene expression and cellular development. Eukaryot. Cell **1:**673–686.
58. **Kono, N., T. Inoue, Y. Yoshida, H. Sato, T. Matsusue, H. Itabe, E. Niki, J. Aoki, and H. Arai.** 2008. Protection against oxidative stress-induced hepatic injury by intracellular type II platelet-activating factor acetylhydrolase by metabolism of oxidized phospholipids in vivo. J. Biol. Chem. **283:**1628–1636.
59. **Kulmburg, P., M. Mathieu, C. Dowzer, J. Kelly, and B. Felenbok.** 1993. Specific binding sites in the *alcR* and *alcA* promoters of the ethanol regulon for the CREA repressor mediating carbon catabolite repression in *Aspergillus nidulans*. Mol. Microbiol. **7:**847–857.
60. **Levin, D. E.** 2005. Cell wall integrity signaling in *Saccharomyces cerevisiae*. Microbiol. Mol. Biol. Rev. **69:**262–291.
61. **Loewith, R., E. Jacinto, S. Wullschleger, A. Lorberg, J. L. Crespo, D. Bonenfant, W. Oppliger, P. Jenoe, and M. N. Hall.** 2002. Two TOR complexes, only one of which is rapamycin sensitive, have distinct roles in cell growth control. Mol. Cell **10:**457–468.
62. **Malavazi, I., M. Savoldi, M. da Silva Ferreira, F. Soriani, P. Bonato, M. de Souza Goldman, and G. Goldman.** 2007. Transcriptome analysis of the *Aspergillus nidulans* AtmA (ATM, Ataxia-Telangiectasia mutated) null mutant. Mol. Microbiol. **66:**74–99.
63. **Matsuo, T., Y. Otsubo, J. Urano, F. Tamanoi, and M. Yamamoto.** 2007. Loss of the TOR kinase Tor2 mimics nitrogen starvation and activates the sexual development pathway in fission yeast. Mol. Cell. Biol. **27:**3154–3164.
64. **McIntyre, M., C. Muller, J. Dynesen, and J. Nielsen.** 2001. Metabolic engineering of the morphology of *Aspergillus*. Adv. Biochem. Eng. Biotechnol. **73:**103–128.
65. **Meyer, V., M. Arentshorst, A. El-Ghezal, A. C. Drews, R. Kooistra, C. A. M. J. J. van den Hondel, and A. F. Ram.** 2007. Highly efficient gene targeting in the *Aspergillus niger kusA* mutant. J. Biotechnol. **128:**770–775.
66. **Meyer, V., M. Arentshorst, C. van den Hondel, and A. Ram.** 2008. The polarisome component SpaA localises to hyphal tips of *Aspergillus niger* and is important for polar growth. Fungal Genet. Biol. **45:**152–164.
67. **Meyer, V., R. A. Damveld, M. Arentshorst, U. Stahl, C. A. van den Hondel, and A. F. Ram.** 2007. Survival in the presence of antifungals: genome-wide expression profiling of *Aspergillus niger* in response to sublethal concentrations of caspofungin and fenpropimorph. J. Biol. Chem. **282:**32935–32948.
68. **Momany, M.** 2001. Molecular and cellular biology of filamentous fungi: a

practical approach, p. 119–125. Oxford University Press, Oxford, United Kingdom.

69. **Mulet, J., D. Martin, R. Loewith, and M. Hall.** 2006. Mutual antagonism of target of rapamycin and calcineurin signaling. J. Biol. Chem. **281:**33000–33007.
70. **Murray, J., and D. Johnson.** 2000. Isolation and characterization of Nrf1p, a novel negative regulator of the Cdc42p GTPase in *Schizosaccharomyces pombe*. Genetics **154:**155–165.
71. **Osmani, A. H., B. R. Oakley, and S. A. Osmani.** 2006. Identification and analysis of essential *Aspergillus nidulans* genes using the heterokaryon rescue technique. Nat. Protoc. **1:**2517–2526.
72. **Papagianni, M.** 2004. Fungal morphology and metabolite production in submerged mycelial processes. Biotechnol. Adv. **22:**189–259.
73. **Pel, H. J., J. H. de Winde, D. B. Archer, P. S. Dyer, G. Hofmann, P. J. Schaap, G. Turner, R. P. de Vries, R. Albang, K. Albermann, M. R. Andersen, J. D. Bendtsen, J. A. Benen, M. van den Berg, S. Breestraat, M. X. Caddick, R. Contreras, M. Cornell, P. M. Coutinho, E. G. Danchin, A. J. Debets, P. Dekker, P. W. van Dijck, A. van Dijk, L. Dijkhuizen, A. J. Driessen, C. d'Enfert, S. Geysens, C. Goosen, G. S. Groot, P. W. de Groot, T. Guillemette, B. Henrissat, M. Herweijer, J. P. van den Hombergh, C. A. van den Hondel, R. T. van der Heijden, R. M. van der Kaaij, F. M. Klis, H. J. Kools, C. P. Kubicek, P. A. van Kuyk, J. Lauber, X. Lu, M. J. van der Maarel, R. Meulenberg, H. Menke, M. A. Mortimer, J. Nielsen, S. G. Oliver, M. Olsthoorn, K. Pal, N. N. van Peij, A. F. Ram, U. Rinas, J. A. Roubos, C. M. Sagt, M. Schmoll, J. Sun, D. Ussery, J. Varga, W. Vervecken, P. J. van de Vondervoort, H. Wedler, H. A. Wosten, A. P. Zeng, A. J. van Ooyen, J. Visser, and H. Stam.** 2007. Genome sequencing and analysis of the versatile cell factory *Aspergillus niger* CBS 513.88. Nat. Biotechnol. **25:**221–231.
74. **Peterbauer, C. K., D. Litscher, and C. P. Kubicek.** 2002. The *Trichoderma atroviride seb1* (stress response element binding) gene encodes an AGGGG-binding protein which is involved in the response to high osmolarity stress. Mol. Genet. Genomics **268:**223–231.
75. **Punt, P. J., and C. A. van den Hondel.** 1992. Transformation of filamentous fungi based on hygromycin B and phleomycin resistance markers. Methods Enzymol. **216:**447–457.
76. **Reinke, A., S. Anderson, J. McCaffery, J. r. Yates, S. Aronova, S. Chu, S. Fairclough, C. Iverson, K. Wedaman, and T. Powers.** 2004. TOR complex 1 includes a novel component, Tco89p (YPL180w), and cooperates with Ssd1p to maintain cellular integrity in *Saccharomyces cerevisiae*. J. Biol. Chem. **279:**14752–14762.
77. **Reynaga-Peña, C. G., and S. Bartnicki-Garcia.** 1997. Apical branching in a temperature sensitive mutant of *Aspergillus niger*. Fungal Genet. Biol. **22:** 153–167.
78. **Reynaga-Peña, C. G., and S. Bartnicki-Garcia.** 2005. Cytoplasmic contractions in growing fungal hyphae and their morphogenetic consequences. Arch. Microbiol. **183:**292–300.
79. **Reynaga-Peña, C. G., G. Gierz, and S. Bartnicki-Garcia.** 1997. Analysis of the role of the Spitzenkörper in fungal morphogenesis by computer simulation of apical branching in *Aspergillus niger*. Proc. Natl. Acad. Sci. USA **94:**9096–9101.
80. **Riquelme, M., S. Bartnicki-Garcia, J. M. Gonzalez-Prieto, E. Sanchez-Leon, J. A. Verdin-Ramos, A. Beltran-Aguilar, and M. Freitag.** 2007. Spitzenkörper localization and intracellular traffic of GFP-labeled CHS-3 and CHS-6 chitin synthases in living hyphae of *Neurospora crassa*. Eukaryot. Cell **6:**1853–1864.
81. **Ruepp, A., A. Zollner, D. Maier, K. Albermann, J. Hani, M. Mokrejs, I. Tetko, U. Guldener, G. Mannhaupt, M. Munsterkotter, and H. W. Mewes.** 2004. The FunCat, a functional annotation scheme for systematic classification of proteins from whole genomes. Nucleic Acids Res. **32:**5539–5545.
82. **Sambrook, J., and D. W. Russel.** 2001. Molecular cloning: a laboratory manual. Cold Spring Harbor Laboratory Press, New York, NY.
83. **Santarius, M., C. H. Lee, and R. A. Anderson.** 2006. Supervised membrane swimming: small G-protein lifeguards regulate PIPK signalling and monitor intracellular PtdIns(4,5)P2 pools. Biochem. J. **398:**1–13.
84. **Schmidt, A., J. Kunz, and M. Hall.** 1996. TOR2 is required for organization of the actin cytoskeleton in yeast. Proc. Natl. Acad. Sci. USA **93:**13780–13785.
85. **Schmitz, H. P., A. Kaufmann, M. Kohli, P. P. Laissue, and P. Philippsen.** 2006. From function to shape: a novel role of a formin in morphogenesis of the fungus *Ashbya gossypii*. Mol. Biol. Cell **17:**130–145.
86. **Schroder, W. A., M. Buck, N. Cloonan, J. F. Hancock, A. Suhrbier, T. Sculley, and G. Bushell.** 2007. Human Sin1 contains Ras-binding and pleckstrin homology domains and suppresses Ras signalling. Cell Signal. **19:** 1279–1289.
87. **Seiler, S., and M. Plamann.** 2003. The genetic basis of cellular morphogenesis in the filamentous fungus *Neurospora crassa*. Mol. Biol. Cell **14:** 4352–4364.
88. **Semighini, C., and S. Harris.** 2008. Regulation of apical dominance in *Aspergillus nidulans hyphae* by reactive oxygen species. Genetics **179:**1919–1932.
89. **Sharpless, K. E., and S. D. Harris.** 2002. Functional characterization and localization of the *Aspergillus nidulans* formin SEPA. Mol. Biol. Cell **13:** 469–479.
90. **Sone, T., and A. J. Griffiths.** 1999. The frost gene of *Neurospora crassa* is a homolog of yeast cdc1 and affects hyphal branching via manganese homeostasis. Fungal Genet. Biol. **28:**227–237.
91. **Spielvogel, A., H. Findon, H. N. Arst, L. Araujo-Bazan, P. Hernandez-Ortiz, U. Stahl, V. Meyer, and E. A. Espeso.** 2008. Two zinc finger transcription factors, CrzA and SltA, are involved in cation homoeostasis and detoxification in *Aspergillus nidulans*. Biochem. J. **414:**419–429.
92. **Steinberg, G.** 2007. Hyphal growth: a tale of motors, lipids, and the Spitzenkörper. Eukaryot. Cell **6:**351–360.
93. **Subramanian, A., P. Tamayo, V. K. Mootha, S. Mukherjee, B. L. Ebert, M. A. Gillette, A. Paulovich, S. L. Pomeroy, T. R. Golub, E. S. Lander, and J. P. Mesirov.** 2005. Gene set enrichment analysis: a knowledge-based approach for interpreting genome-wide expression profiles. Proc. Natl. Acad. Sci. USA **102:**15545–15550.
94. **Taheri-Talesh, N., T. Horio, L. Araujo-Bazán, X. Dou, E. Espeso, M. Peñalva, S. Osmani, and B. Oakley.** 2008. The tip growth apparatus of *Aspergillus nidulans*. Mol. Biol. Cell **19:**1439–1449.
95. **Takeshita, N., A. Ohta, and H. Horiuchi.** 2005. CsmA, a class V chitin synthase with a myosin motor-like domain, is localized through direct interaction with the actin cytoskeleton in *Aspergillus nidulans*. Mol. Biol. Cell **16:**1961–1970.
96. **Thykaer, J., K. Rueksomtawin, H. Noorman, and J. Nielsen.** 2009. Disruption of the NADPH-dependent glutamate dehydrogenase affects the morphology of two industrial strains of *Penicillium chrysogenum*. J. Biotechnol. **139:**280–282.
97. **Torralba, S., and I. B. Heath.** 2001. Cytoskeletal and Ca^{2+} regulation of hyphal tip growth and initiation. Curr. Top. Dev. Biol. **51:**135–187.
98. **van Hartingsveldt, W., I. E. Mattern, C. M. van Zeijl, P. H. Pouwels, and C. A. van den Hondel.** 1987. Development of a homologous transformation system for *Aspergillus niger* based on the *pyrG* gene. Mol. Gen. Genet. **206:**71–75.
99. **van Loon, A., B. Pesold-Hurt, and G. Schatz.** 1986. A yeast mutant lacking mitochondrial manganese-superoxide dismutase is hypersensitive to oxygen. Proc. Natl. Acad. Sci. USA **83:**3820–3824.
100. **Vieira, J., and J. Messing.** 1991. New pUC-derived cloning vectors with different selectable markers and DNA replication origins. Gene **100:**189–194.
101. **Virag, A., and A. J. Griffiths.** 2004. A mutation in the *Neurospora crassa* actin gene results in multiple defects in tip growth and branching. Fungal Genet. Biol. **41:**213–225.
102. **Virag, A., and S. D. Harris.** 2006. Functional characterization of *Aspergillus nidulans* homologues of *Saccharomyces cerevisiae* Spa2 and Bud6. Eukaryot. Cell **5:**881–895.
103. **Wang, G., L. Lu, C. Y. Zhang, A. Singapuri, and S. Yuan.** 2006. Calmodulin concentrates at the apex of growing hyphae and localizes to the Spitzenkörper in *Aspergillus nidulans*. Protoplasma **228:**159–166.
104. **Wang, S. Z., and R. M. Roberts.** 2005. The evolution of the Sin1 gene product, a little known protein implicated in stress responses and type I interferon signaling in vertebrates. BMC Evol. Biol. **5:**13.
105. **Wilkinson, M. G., T. S. Pino, S. Tournier, V. Buck, H. Martin, J. Christiansen, D. G. Wilkinson, and J. B. Millar.** 1999. Sin1: an evolutionarily conserved component of the eukaryotic SAPK pathway. EMBO J. **18:**4210–4221.
106. **Wongwicharn, A., B. McNeil, and L. M. Harvey.** 1999. Effect of oxygen enrichment on morphology, growth, and heterologous protein production in chemostat cultures of *Aspergillus niger* B1-D. Biotechnol. Bioeng. **65:**416–424.
107. **Wösten, H. A., M. S. Moukha, J. H. Sietsma, and J. G. Wessels.** 1991. Localisation of growth and secretion of proteins in *Aspergillus niger*. J. Gen. Microbiol. **137:**2017–2023.
108. **Wright, G. D., J. Arlt, W. C. Poon, and N. D. Read.** 2007. Optical tweezer micromanipulation of filamentous fungi. Fungal Genet. Biol. **44:**1–13.
109. **Wullschleger, S., R. Loewith, W. Oppliger, and M. Hall.** 2005. Molecular organization of target of rapamycin complex 2. J. Biol. Chem. **280:**30697–30704.
110. **Yang, Q., K. Inoki, T. Ikenoue, and K. L. Guan.** 2006. Identification of Sin1 as an essential TORC2 component required for complex formation and kinase activity. Genes Dev. **20:**2820–2832.
111. **Zheng, X. D., Y. M. Wang, and Y. Wang.** 2003. CaSPA2 is important for polarity establishment and maintenance in *Candida albicans*. Mol. Microbiol. **49:**1391–1405.
112. **Ziv, C., R. Gorovits, and O. Yarden.** 2008. Carbon source affects PKA-dependent polarity of *Neurospora crassa* in a CRE-1-dependent and independent manner. Fungal Genet. Biol. **45:**103–116.